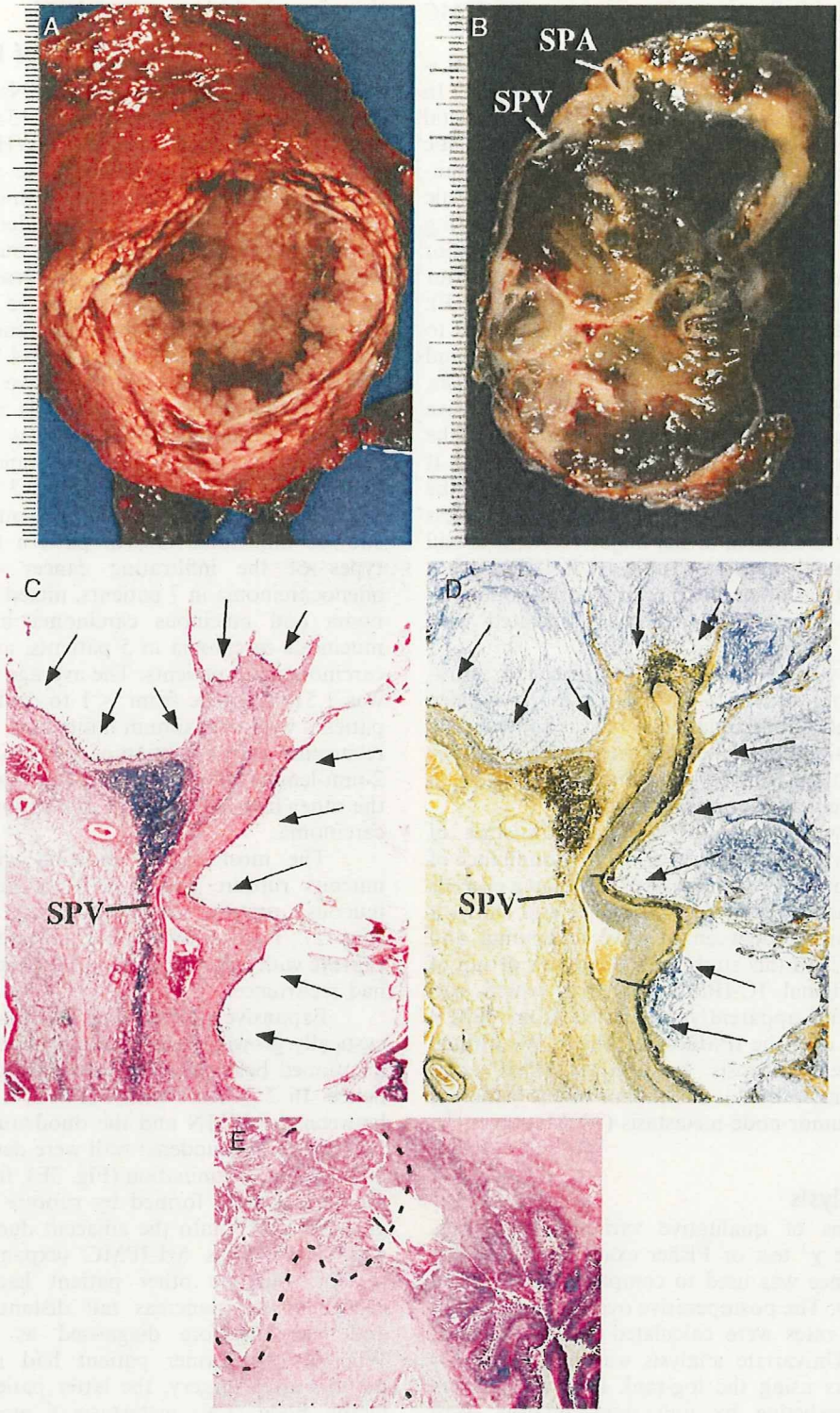

FIGURE 3. Histopathologic features of "expansive growth" in I-IPMC. The pancreatic duct is markedly dilated to a cystlike shape (A, B). Fresh cut view (A) and formalin-fixed cut surface (B) of cystic I-IPMCs. Cystically dilated pancreatic duct is filled with clear mucus and many papillary projections are seen on the inner surface (A). The SPV is compressed (B–D) and its thickened wall is eroded by an enlarged cystic IPMC (arrows) in hematoxylin and eosin stain (C) and elastica stain (D). A fistula has been formed between cystic I-IPMC (dotted line) and duodenum (E).

All of the 24 patients with mucous rupture MI-IPMC survived after surgery.

Expansive growth of ductectatic or cystic IPMN is another characteristic feature of IPMN (Fig. 3). In addition to mucous rupture, an increase of intraductal pressure by hypersecretion of mucus causes marked cystic dilatation of the duct, which continues to grow expansively into extrapancreatic tissue. In some cases, cystic IPMC eventually forms a fistula with surrounding digestive organs (Fig. 3E) or erodes the wall of major blood vessels [portal vein, splenic vein (SPV), superior mesenteric vein (SMV), or splenic artery] (Figs. 3C–E). Such growth and spread are rather passive in contrast to the infiltrative growth that occurs in active invasion and this feature was not associated with poor prognosis, similarly to mucous rupture. IPMC showing expansive growth with loss of the basement membrane of the pancreatic duct in the IPMC is diagnosed as MI-IPMC. If I-IPMC grows expansively, even if it ruptures into the bowel, or even if it erodes a major vessel wall unless cancer cells enter the lumen of the major vessel, it is still regarded as minimal invasion (Table 1). If I-IPMC has this type of growth as predominance, it is corresponded to a kind of pure mucinous carcinoma associated with IPMC.

Although we have not yet experienced intra-abdominal rupture of IPMC, a few cases have been reported.[18] As intra-abdominal rupture was followed by peritoneal dissemination in these reported cases, this type should be distinguished from ordinary IPMN and managed separately as ruptured IPMN.

IC-IPMC was defined as a lesion consisting of IPMN and invasive carcinoma with the predominance of the IPMN component.[12] Such invasive carcinoma exceeds the minimal invasion proposed in Table 1, and shows a continuous transition between invasive carcinoma and intraductal IPMC. In this study, we added new group of cases to the original IC-IPMC category, which had invasive carcinoma apparently originated from IPMN but predominant over the IPMN component. We wanted to compare the prognosis between IC-IPMC and conventional invasive ductal carcinoma of the pancreas in the matched tumor-node-metastasis (TNM) stages.[11]

Statistical Analysis

Comparisons of qualitative variables were performed using the χ^2 test or Fisher exact test. One-way analysis of variance was used to compare the means of 3 or more groups. The postoperative overall and disease-specific survival rates were calculated by the Kaplan-Meier method. Univariate analysis was performed for prognostic factors using the log-rank test. The factors found to be predictive by univariate analysis were subjected to multivariate analysis using the Cox proportional hazards model. Differences at $P < 0.05$ were considered statistically significant. Statistical analyses were performed with SPSS 11.0J software (SPSS Inc, Chicago, IL).

RESULTS

Histopathologic Evaluation of I-IPMC

One hundred and four IPMNs were classified into 27 IPMAs, 11 borderline IPMNs, 15 noninvasive IPMCs, and 51 I-IPMCs according to the WHO classification.[13,15] None of them had an ovarianlike stroma, and all the lesions showed communication with the pancreatic ductal system. I-IPMCs were further divided into 26 MI-IPMCs and 25 IC-IPMCs according to our criteria (Table 1) based on the histopathologic pattern of invasion.

To evaluate the aggressive characteristics of I-IPMC, we examined the invasiveness of I-IPMC. The invasiveness was categorized into 4 patterns: infiltrative growth, mucous rupture, expansive growth, and intra-abdominal rupture (see Materials and Methods). The criterion of minimal invasion was proposed for each corresponding pattern (Table 1), and the representative features are shown in Figures 1 to 3.

Seventeen among 26 patients with MI-IPMC showed infiltrative growth pattern (Fig. 1). Histologic types of the infiltrating cancer cells were tubular adenocarcinoma in 7 patients, mixed tubular adenocarcinoma and mucinous carcinoma in 2 patients, pure mucinous carcinoma in 5 patients, and papillary adenocarcinoma in 3 patients. The average depth of infiltration was 1.5 mm (range from < 1 to 5 mm). None of the 17 patients with a maximum infiltration of 5 mm or less had recurrence with exception of 2 patients, one of them had 2-mm-length infiltration of tubular adenocarcinoma and the other had 2-mm-length infiltration of pure mucinous carcinoma.

The most of the patients with MI-IPMC had mucous rupture and 6 patients had MI-IPMC with mucous rupture as predominant invasive pattern (Fig. 2). Two of them were subcategorized as mucous rupture with cellular component. None of these 6 patients had recurrence.

Expansive growth (Fig. 3) was often observed in cystically growing tumors and 4 patients with MI-IPMC mentioned below showed expansive growth as predominance. In 2 patients with I-IPMC, a fistula was formed between the IPMN and the duodenum. No cancer cells infiltrating the duodenal wall were detected in either case by histologic examination (Fig. 3E). It was suspected that the fistulas were formed by rupture of the expansively growing IPMN into the adjacent duodenum. The lesion was classified as MI-IPMC (expansive growth) in 1 patient, but the other patient had definite invasive cancer in the pancreas tail distant from the fistula, and was therefore diagnosed as having IC-IPMC. Whereas the former patient had no recurrence 107 months after surgery, the latter patient developed local lymph node (LN) metastasis 6 months after surgery and died of the disease. In the other 3 patients with expansive growth of MI-IPMC, the IPMN had grown deeply into the retropancreatic tissue, compressing the wall of the SPV or SMV. In one of them, the tunica media of the SPV was involved without a fistula

TABLE 2. Comparison of Invasive Lesion Between MI-IPMC and IC-IPMC

	MI-IPMC (n = 26)	IC-IPMC (n = 25)	P*
Growth pattern			
Infiltrative growth	17	25	
Mucous rupture or expansive growth as predominance	10†	0	
Vessel or neural invasion	4	25	**< 0.001**
Lymphatic invasion	0	23	**< 0.001**
Venous invasion	2	24	**< 0.001**
Intrapancreatic neural invasion	2	22	**< 0.001**
Extrapancreatic involvement	4	23	**< 0.001**
Serosa	0	4	0.051
Retropancreatic tissue	3‡	21	**< 0.001**
Duodenum	1‡	8	**0.002**
Extrahepatic bile duct	0	3	0.110
Portal venous system	1‡	8	**0.011**
Arterial system	0	1	0.490
Extrapancreatic nerve plexus	0	4	0.051
Invasion to surgical margin	0	4	0.051
Metastasis	0	17	**< 0.001**
Local LN	0	17	**< 0.001**
Distant organs	0	4§	0.051
TNM stage			**< 0.001**
IA	22	1	
IB	0	0	
IIA	4	7	
IIB	0	13	
III	0	0	
IV	0	4§	
Histology of infiltrative growth			
Pap	3	2	
Tub1	7	5	
Tub2	0	8	
Tub+Muc	2	7	
Tub3	0	1	
Muc	5	1	
AS	0	1	

Statistically significant value is in bold characters.

*P value was calculated by χ^2 or Fisher exact test.

†6 patients showed mucous rupture (2 of them showed mucous rupture with cellular component) and 4 patients showed expansive growth (one of them showed infiltrative growth as well).

‡Due to expansive growth.

§One patient with liver metastasis, 3 patients with para-aortic LN metastasis.

AS indicates adenosquamous carcinoma; Muc, mucinous carcinoma; Pap, papillary adenocarcinoma; Tub1, well-differentiated tubular adenocarcinoma; Tub2, moderately differentiated tubular adenocarcinoma; Tub3, poorly differentiated tubular adenocarcinoma.

between tumor and SPV (Figs. 3C–E). These 3 patients did not have postoperative recurrence at 28, 52, and 96 months after surgery, respectively. We thought mucous rupture and expansive growth is dormant invasion, considering its nonaggressive nature, which is characteristic to IPMN.

Comparison of the pathologic characteristics and TNM staging[11] between invasive lesions of MI-IPMCs and IC-IPMCs are summarized in Table 2. Vessel or neural invasion and extrapancreatic involvement were much more common in IC-IPMC than in MI-IPMC. No LN metastasis was observed in patients with MI-IPMC, whereas 17 patients (68%) with IC-IPMC showed LN metastasis. With regard to the histology of the invasive component of the IC-IPMC, most of the patients had tubular adenocarcinoma and only 1 patient had pure mucinous carcinoma. Among 26 patients with MI-IPMC, 9 had tubular adenocarcinoma and 11 had pure mucinous carcinoma.

Prognostic Significance of the Classification of I-IPMC

The median survival period for the 104 patients was 142 months, and the 3, 5, and 10-year overall survival rates were 86%, 78%, and 59%, respectively. There was no statistically significant difference in overall survival among patients with IPMA, borderline IPMN, and noninvasive IPMC ($P = 0.54$). Therefore, they were integrated into noninvasive IPMN for subsequent analysis. The survival rates 3, 5, and 10 years after surgery were 95%, 92%, and 70% for noninvasive IPMN, 95%, 79%, and 79% for MI-IPMC, and 51%, 38%, and 0% for IC-IPMC (Fig. 4A). The disease-specific survival rates after 3, 5, and 10 years were 100%, 100%, and 100% for noninvasive IPMN, 100%, 100%, and 100% for MI-IPMC, and 51%, 38%, and 0% for IC-IPMC (Fig. 4B). Overall and disease-specific survival for MI-IPMC was significantly better than for IC-IPMC ($P < 0.001$), whereas there was no significant difference in overall survival between noninvasive IPMN and MI-IPMC ($P = 0.66$).

Overall survival was compared between I-IPMC and conventional invasive ductal carcinoma of the pancreas during the same period (Figs. 5A–D). The stages of IC-IPMCs were assessed on the basis of size and spread of invasive carcinoma in the lesion, using the International Union against Cancer (UICC) TNM classification,[11] and classified as stage IA, IB, and IIA, stage IIB, and stage III and IV. Between IC-IPMC and conventional invasive ductal carcinoma of the pancreas at each corresponding TNM stage, there was no statistically significant difference in survival rate, though IC-IPMC had a tendency to show a favorable outcome.

Prognostic Factors in I-IPMCs

Clinicopathologic factors possibly affecting the postoperative outcome of I-IPMCs were studied (Table 3). The following variables were significantly related to unfavorable prognosis: presence of jaundice, cancer cells present at the surgical margin except the pancreatic margin, presence of major vascular invasion [portal vein, SMV, SPV, or splenic artery], presence of lymphatic invasion, presence of venous invasion, presence of intrapancreatic neural invasion, presence of LN metastasis, presence of para-aortic LN metastasis, CA19-9 > 300 U/mL, size of invasive cancer > 2 cm, histopathologic diagnosis of IC-IPMC (vs. MI-IPMC), and tubular adenocarcinoma as histologic type of invasive cancer in I-IPMC. Multivariate analysis (backward elimination method) showed that a histopathologic diagnosis of I-IPMC classified as IC-IPMC and

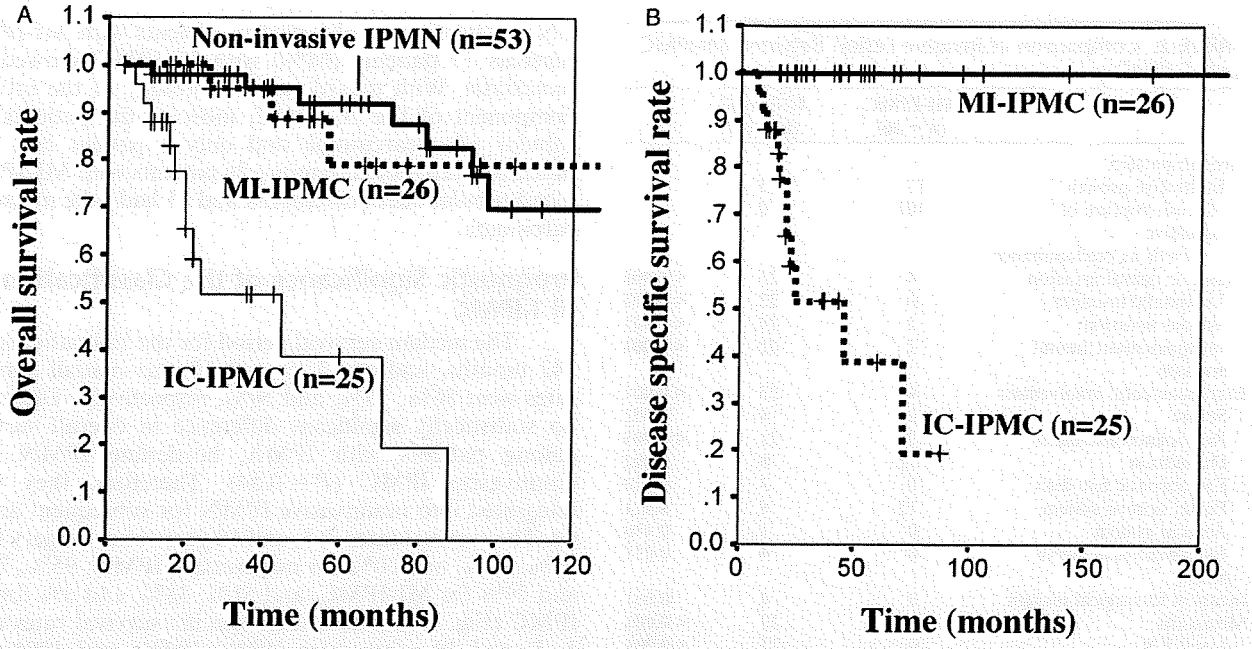

FIGURE 4. Kaplan-Meier survival curves of the 104 patients with IPMNs. A, Overall survival of patients with MI-IPMC was significantly better than that of patients with IC-IPMC ($P<0.001$), whereas no significant difference was found between patients with noninvasive IPMN and those with MI-IPMC ($P=0.66$). B, Disease-specific survival of patients with MI-IPMC was significantly better than that of patients with IC-IPMC ($P<0.001$), with no disease-related death among 26 patients with MI-IPMC during a median follow-up period of 43.4 (13.2 to 210) months.

CA19-9 > 300 U/mL were significant prognostic factors (Table 4).

Postoperative Recurrence of IPMNs

Postoperative recurrence was observed in 15 patients exclusively among those with I-IPMC (Table 5). Two patients with MI-IPMC suffered recurrence of MI-IPMC and invasive cancer in the remnant pancreas 36 and 48 months after surgery, respectively. At initial surgery, both patients had undergone PPPD for IPMNs in the pancreas head with negative surgical margins. The former underwent completion pancreatectomy in a second operation, and pathologic examination revealed another MI-IPMC in the remnant pancreas distant from the site of pancreato-jejunostomy. In the latter patient, recurrence of invasive ductal carcinoma was also found distant from the pancreato-jejunostomy, and additional partial resection of the remnant pancreas was performed. Both patients are currently doing well with no evidence of recurrence 8 and 20 months after the second operation, respectively. The remaining 13 recurrences were observed in patients with IC-IPMC. The site of recurrence was local (remnant pancreas) in 2 patients, LN in 2 patients, the lung in 1 patient, the liver in 4 patients, and peritoneal dissemination in 4 patients (Table 5). The time interval between surgery and recurrence was less than 20 months in all cases, with an especially short duration of 6.15 ± 0.82 months for patients with peritoneal dissemination.

Analysis of the Pancreatic Surgical Margin

Intraoperative frozen section analysis of the pancreas margin was performed in 96 patients, and 17 patients needed additional pancreatic resection owing to the confirmed or suspected presence of cancer cells at the pancreatic surgical margin (Table 5). Additional resection was performed more frequently in patients with MI-IPMC and IC-IPMC than in those with noninvasive IPMN, regardless of IPMN size ($P = 0.007$). The final pancreatic margin status was negative in 75 patients, positive for IPMA in 25, borderline IPMN in 2, noninvasive IPMC in 1, and invasive carcinoma in 1.

DISCUSSION

Many groups have investigated the malignant potential of IPMNs,[4,6,16,20,22–24] and the recent consensus is that its aggressiveness is dependent on the presence of invasive cancer, the extent of cancer invasion, and the biologic characteristics of the cancer cells.[2,3,8,10,14,15] However, no sufficient pathologic and presurgical staging system has yet been established for evaluating the malignant potential of I-IPMC. In this study, we examined 104 IPMNs surgically resected at the same hospital and proposed histopathologic criteria for classification of I-IPMC. I-IPMC shows heterogeneous features, which reflect the presence of heterogeneous cancer types with different biologic behaviors. Therefore, the criteria of MI-IPMC should differ in accordance with each histopathologic pattern of invasion. Our proposed

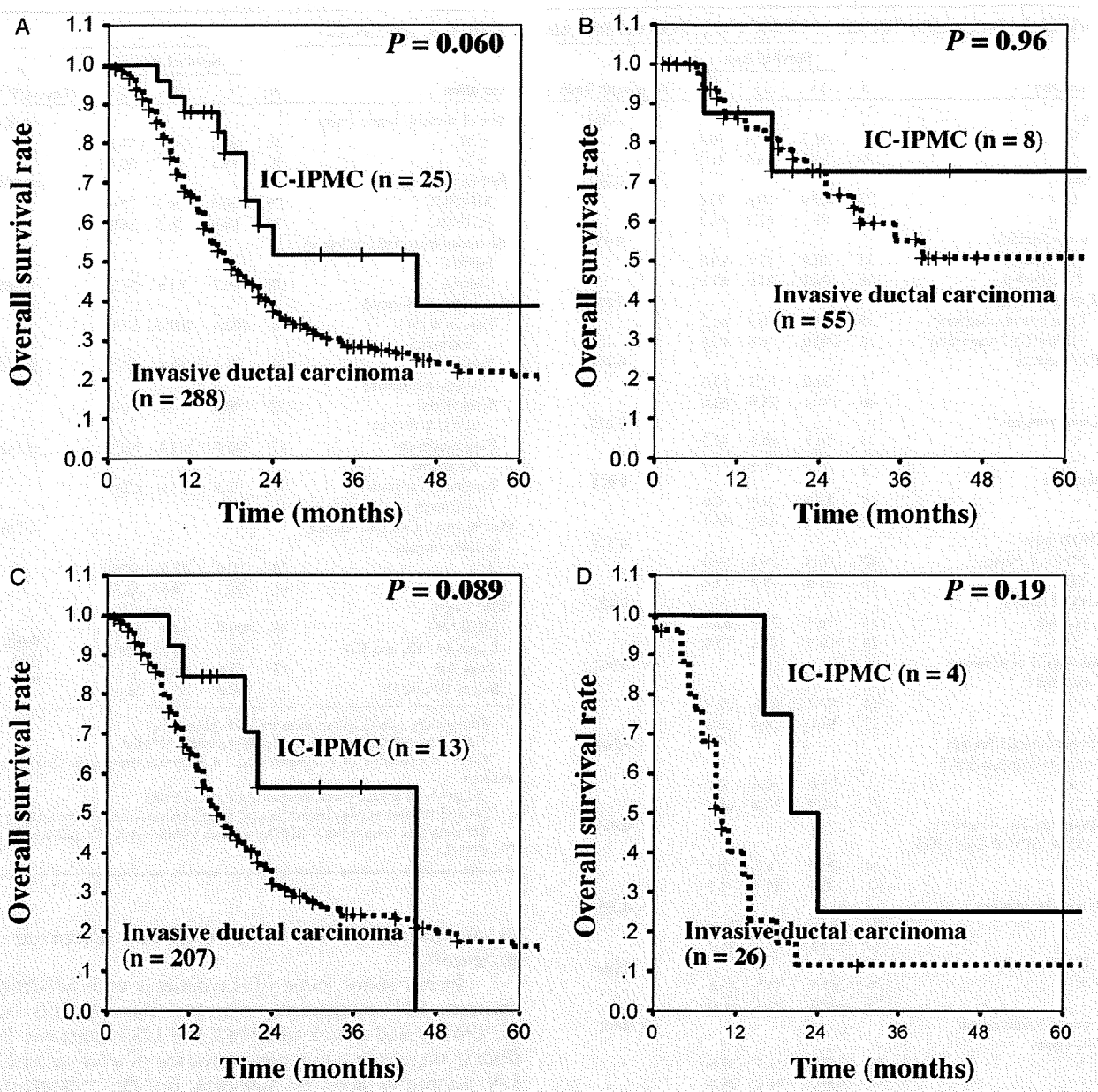

FIGURE 5. Kaplan-Meier survival curves of the 25 patients with IC-IPMC and the 288 patients with invasive ductal carcinoma of the pancreas. Comparison of overall survival of the patients with IC-IPMC and that of patients with conventional invasive ductal carcinoma at all stages (A), and in stage IA, IB, and IIA (B), stage IIB (C), and stage III and IV (D). Although the patients with IC-IPMC tended to have a better outcome than those with conventional invasive ductal carcinoma at each corresponding stage, the difference was not statistically significant.

criteria of invasiveness were successful in categorizing IPMCs in our series into noninvasive IPMC, MI-IPMC, and IC-IPMC. Patients with IC-IPMC had a significantly worse outcome than those with MI-IPMC. However, there was no difference in postoperative outcome between patients with MI-IPMC and those with noninvasive IPMC. This is the first report to propose practical criteria for MI-IPMC that can separate early-stage nonaggressive I-IPMC from total I-IPMC. Discrimination between MI-IPMC and IC-IPMC can provide important information for predicting the postoperative outcome of patients with IPMNs and also for deciding additional clinical management.

When IC-IPMCs were staged according to the size and spread of an invasive carcinoma component, the survival curve showed a similar decline to that of conventional invasive ductal carcinomas of the corresponding TNM stage, suggesting that it is the invasive

TABLE 3. Prognositic Factors of I-IPMCs in Univariate Analysis

Variables	n	Survival Rate 1 y	3 y	5 y	P (Log-rank Test)
Sex					0.262
M	27	96.3	80.4	80.4	
F	24	91.7	70.4	41.5	
Age (y)					0.082
≤70	33	100.0	80.6	72.6	
> 70	18	83.3	67.3	46.2	
Tumor location					0.937
Ph included	33	93.9	72.4	60.8	
Ph excluded	18	94.4	84.0	67.2	
Tumor distribution					0.821
Confined in 1 segment	35	91.4	75.7	63.2	
Diffuse (≥2 segments)	16	100.0	76.6	63.8	
PV resection					0.471
+	5	80.0	53.3	53.3	
–	46	95.7	78.0	63.0	
Chief complaint*					0.225
+	28	92.9	65.6	49.2	
–	23	95.6	90.0	81.0	
Jaundice					**0.011**
+	6	83.3	27.8	0.0	
–	45	95.6	80.7	66.2	
IPMN type					0.571
MPD or mixed	40	97.5	76.2	59.0	
BD	11	81.8	72.7	72.7	
MPD diameter					0.422
≤8 mm	31	90.3	75.4	52.2	
> 8 mm	20	100.0	75.6	75.6	
Additional resection of pancreas†					0.864
+	14	92.9	63.7	63.7	
–	37	94.6	78.4	60.3	
Surgical margin (except for pancreas margin)‡					**< 0.001**
+ or ±	4	75.0	0.0	0.0	
–	47	95.7	84.4	69.1	
Major vascular invasion (SMV, SPV, PV, or SPA)					**0.009**
+	10	90.0	48.2	0.0	
–	41	95.1	82.0	71.2	
Lymphatic invasion					**< 0.001**
+	23	87.0	44.7	22.4	
–	28	100.0	95.5	81.7	
Venous invasion					**0.006**
+	26	88.5	53.5	42.8	
–	25	100.0	94.4	78.0	
Intrapancreatic neural invasion					**< 0.001**
+	24	87.5	52.7	39.5	
–	27	100.0	94.4	78.4	
Local LN metastasis					**< 0.001**
+	18	88.9	47.1	23.5	
–	33	97.0	88.9	76.4	
Para-aortic LN metastasis					**< 0.001**
+	3	100.0	0.0	0.0	
–	48	93.8	32.3	67.4	
CEA (ng/mL)					0.455
≤5	35	94.3	83.4	64.3	
> 5	16	93.8	58.4	58.4	
CA19-9 (U/mL)					**< 0.001**
≤300	40	97.5	84.5	79.8	
> 300	11	81.8	40.9	0.0	
IPMN size (mm)					0.552
≤40	15	93.3	70.2	43.9	
> 40	36	94.4	78.2	72.2	
IPMN size (mm)					0.762
≤70	33	90.9	74.8	60.0	
> 70	18	100.0	77.0	66.0	
Size of invasive lesion (mm)					0.001
≤20	32	96.9	88.7	75.1	
> 20	19	89.5	48.7	32.4	
Pathologic diagnosis					**< 0.001**
MI-IPMC	26	100.0	94.7	78.6	
IC-IPMC	25	88.0	50.6	38.0	
Histology of invasive cancer in I-IPMC					
Tubular adenocarcinoma§	29	89.7	61.8	54.1	0.065
Pure mucinous carcinoma	12	100.0	100.0	57.1	
Tubular adenocarcinoma§	29	89.7	61.8	54.1	**0.010**
Nontubular adenocarcinoma	22	100.0	94.4	71.6	
Pure mucinous carcinoma	12	100.0	100.0	57.1	0.162
Nonpure mucinous carcinoma	39	92.3	68.6	62.9	
Past history of another cancer in other organs					0.316
+	10	90.0	72.0	54.0	
–	41	95.1	79.8	63.3	
TNM stage					
MI-IPMC	26	100.0	94.7	78.6	
Stages IA, IB, and IIA	8	87.5	70.0	70.0	**0.040**
Stage IIB	13	84.6	56.4	0.0	0.42
Stages III and IV	4	100.0	25.0	25.0	0.82

Statistically significant value is in bold characters.
*Diabetes mellitus exacerbation and jaundice included.
†Due to existence of neoplastic cells in pancreas margin in frozen section analysis.
‡Presence of invasive carcinoma cells in the stroma.
§Mixed tubular adenocarcinoma and mucinous carcinoma were included.
BD indicates branch duct; MPD, main pancreatic duct; Ph, pancreatic head; PV, portal vein.

carcinoma rather than IPMN itself that determines the prognosis.

In our series, none of the patients with MI-IPMCs showed LN metastasis, whereas the patients with IC-IPMCs had a high rate (68%) of LN metastasis. This finding implies that complete resection of a lesion without LN dissection may be sufficient for the treatment of MI-IPMC, whereas radical pancreatectomy with LN dissection is indicated for IC-IPMC. In this context, preoperative distinction between MI-IPMCs and IC-IPMCs is clinically very important.

TABLE 4. Multivariate Analysis of Effects of Clinicopathologic Factors on Postoperative Survival of I-IPMC

	Hazard Ratio	95% Confidence Interval	P*
IC-IPMC (vs. MI-IPMC)	7.1	1.9-26.5	< 0.001
CA19-9 > 300 (U/mL)	4.4	1.4-13.8	0.010

*P value was calculated by Cox hazards model (backward elimination method).

TABLE 5. Pancreatic Margin Status and the Recurrence of IPMNs After Surgery

	IPMA or Borderline IPMN (n = 38)	Noninvasive IPMC (n = 15)	MI-IPMC (n = 26)	IC-IPMC (n = 25)	Total (n = 104)	P
Additional pancreas resection*	3	0	5	9	17	0.007†
Final margin status						0.071
Negative	26	10	20 (2)	19 (11)	75	
IPMA	12	5	5	3 (1)‡	25	
Borderline IPMN	0	0	1	1	2	
Noninvasive IPMC	0	0	0	1	1	
Invasive cancer	0	0	0	1 (1)§	1	
Recurrence						
MI-IPMC (in the remnant pancreas)	0	0	1	0	1	
Invasive cancer (in the remnant pancreas)	0	0	1	0	1	
Local recurrence of invasive cancer	0	0	0	2	2	
Local LN	0	0	0	2	2	
Distant metastasis (lung or liver)	0	0	0	5	5	
Peritoneal dissemination	0	0	0	4	4	
Total	0	0	2	13	15	

*Due to the presence of neoplastic cells in the pancreatic surgical margin in the frozen section analysis.
†Comparison between noninvasive IPMN and I-IPMC.
‡Liver metastasis.
§Local recurrence, numbers in the parentheses denotes the number of patients who developed recurrence after the operation.

Another significant finding was a predominantly high recurrence rate among patients with IC-IPMC (52%), compared with 2.5% for patients with noninvasive IPMN or MI-IPMC. In the latter group, recurrence was observed in the remnant pancreas distant from the cut end, suggesting that IPMC occurred multifocally. Although this recurrence rate is not as high as that reported previously,[4] careful follow-up seems to be necessary after surgery, especially in patients with IC-IPMCs.

Our criteria are not contradictory to the previous studies, in which the postoperative outcome of I-IPMC with pure mucinous carcinoma (colloid carcinoma) was better than that of patients with I-IPMC with tubular adenocarcinoma in the invasive lesion.[1,24] Tubular adenocarcinoma shows active infiltrative growth similar to conventional pancreatic ductal adenocarcinoma, suggesting that it rapidly grows and progresses into advanced cancer. In fact, tubular adenocarcinoma occurred at a higher rate in IC-IPMC than in MI-IPMC, and was an unfavorable prognostic factor ($P = 0.010$; Table 3). It has been reported that mucinous carcinoma associated with IPMN or mucinous cystic tumor has a better outcome than conventional ductal carcinoma. According to Adsay's criteria (a carcinoma with more than 80% of mucinous carcinoma is defined as pure mucinous carcinoma),[1] 12 I-IPMCs were diagnosed as pure mucinous carcinoma associated with IPMC in our series, which contained 11 MI-IPMC (5 with infiltrative growth of pure mucinous carcinoma, 2 with predominantly mucous rupture with cellular component, and 4 with expansive growth) and 1 IC-IPMC. Among these 12 patients with pure mucinous carcinoma associated with IPMC, 1 patient with MI-IPMC with infiltrative growth and 1 patient with IC-IPMC had recurrence of the carcinoma. Although 12 patients had the recurrent cancers and 10 of them died among 29 patients of I-IPMCs with tubular adenocarcinoma (8 in MI-IPMC and 21 in IC-IPMC). Patients with pure mucinous carcinoma as histologic type of invasive cancer tended to have better prognosis than patients with tubular adenocarcinoma as invasive cancer ($P = 0.065$; Table 3). Our study also suggested that some mucinous carcinoma has aggressive behavior. The prognosis of mucinous carcinoma in the other organs such as colon, has been reported to be worse than the ordinary adenocarcinoma, especially worse for mucinous carcinoma with rich cellular component.[17,21] In ductal carcinoma of the pancreas, mixed mucinous carcinoma with other histologic types of carcinoma (usually tubular adenocarcinoma) shows bad prognosis comparable with the other types of conventional ductal adenocarcinoma.[7,14] In this situation, it is desired that a diagnostic criterion is established to distinguish aggressive and nonaggressive mucinous carcinoma correctly. In this study, addition to the classification of tubular adenocarcinoma of the I-IPMC into aggressive and nonaggressive state, we also classified mucinous carcinoma relevant to clinical behavior based on the invasiveness and cellularity. Compared with mucous rupture, more aggressive mucinous carcinoma shows massive invasion with much more cancer cells floating and proliferating in mucus lakes, and is often accompanied by partial invasion of tubular adenocarcinoma.

Lymphatic, venous, and intrapancreatic neural invasion were frequently observed in IC-IPMC (Table 2) and were significant prognostic factors in I-IPMC (Table 3). In this study, we tried to select early-stage I-IPMC with nonaggressive characters from I-IPMCs with such worse prognostic factors. We successfully selected it by categorizing the infiltrating depth of cancer cells, which included lymphatic, venous, and/or neural invasion. Indeed, all the patients with MI-IPMC having vessel or neural invasion within 5-mm length from IPMC duct

showed good postoperative outcome. In addition, lymphatic, venous, and intrapancreatic neural invasion were not significant variables for the prognosis in multivariate analysis (Table 4).

The present results suggest that IC-IPMC (not MI-IPMC) should be currently paid attention as I-IPMC with aggressive characteristics. In this situation, preoperative detection of IC-IPMC can be beneficial for selecting the most ideal operative procedure, especially on considering additional LN dissection. We are now investigating possible criteria for classifying these cancers preoperatively, and our findings suggest that it may be feasible to use radiologic data for this purpose. Multidetector row computed tomography was found to be useful to distinguish IC-IPMC from MI-IPMC and noninvasive IPMNs with more than 80% sensitivity and 100% specificity in the study using 123 patients with IPMNs (manuscript in preparation).

In future, we would like to test our criteria using another large series of samples or in a prospective study, to obtain more watertight pathologic criteria for classification of I-IPMC.

ACKNOWLEDGMENTS

The authors thank Drs Tsuyoshi Sano, Yoshihiro Sakamoto, Hidenori Ojima, and Minoru Esaki for useful discussions.

REFERENCES

1. Adsay NV, Merati K, Nassar H, et al. Pathogenesis of colloid (pure mucinous) carcinoma of exocrine organs. *Am J Surg Pathol.* 2003; 27:571–578.
2. Adsay NV, Merati K, Basturk O, et al. Pathologically and biologically distinct types of epithelium in intraductal papillary mucinous neoplasms. Delineation of an 'intestinal' pathway of carcinogenesis in the pancreas. *Am J Surg Pathol.* 2004;28:839–848.
3. Biankin AV, Kench JG, Dijkman FP, et al. Molecular pathogenesis of precursor lesions of pancreatic ductal adenocarcinoma. *Pathology.* 2003;35:14–24.
4. Chari ST, Yadav D, Smyrk TC, et al. Study of recurrence after surgical resection of intraductal papillary mucinous neoplasm of the pancreas. *Gastroenterology.* 2002;123:1500–1507.
5. Cho KR, Vogelstein B. Genetic alterations in the adenoma-carcinoma sequence. *Cancer.* 1992;70:1727–1731.
6. D'Angelica M, Brennan MF, Suriawinata AA, et al. Intraductal papillary mucinous neoplasms of the pancreas: an analysis of clinicopathologic features and outcome. *Ann Surg.* 2004;239:400–408.
7. Fukushima N, Mukai K, Kanai Y, et al. Intraductal papillary tumors and mucinous cystic tumors of the pancreas. *Hum Pathol.* 1997;28:1010–1017.
8. Furukawa T, Klöppel G, Volkan Adsay N, et al. Classification of types of intraductal papillary-mucinous neoplasm of the pancreas: a consensus study. *Virchows Arch.* 2005;447:794–799.
9. Hiraoka N, Onozato K, Kosuge T, et al. Prevalence of FOXP3$^+$ regulatory T cells increases during the progression of pancreatic ductal adenocarcinoma and its precursor lesions. *Clin Cancer Res.* 2006;12:5423–5434.
10. Hruban RH, Takaori K, Klimstra DS, et al. An illustrated consensus on the classification of pancreatic intraepithelial neoplasia and intraductal papillary mucinous neoplasms. *Am J Surg Pathol.* 2004;28:977–987.
11. International Union Against Cancer (UICC). *TNM Classification of Malignant Tumors.* 6th ed. New York, NY: Wiley-Liss; 2002.
12. Japan Pancreas Society. *Classification of Pancreatic Cancer.* 2nd ed. Tokyo, Japan: Kanehara; 2003.
13. Klöppel G, Solcia E, Longnecker DS, et al. *Histological Typing of Tumors of the Exocrine Pancreas, World Health Organization International Histological Classification of Tumors.* 2nd ed. Berlin, Germany: Springer; 1996.
14. Klöppel G, Hruban RH, Longnecker DS, et al. Ductal adenocarcinoma of the pancreas. In: Hamilton SR, Aaltonen LA, eds. *Pathology and Genetics. Tumours of the Digestive System. World Health Organization Classification of Tumours.* Lyon, France: IARC Press; 2000:221–230.
15. Longnecker DS, Adler G, Hruban RH, et al. Intraductal papillary-mucinous neoplasms of the pancreas. In: Hamilton SR, Aaltonen LA, eds. *Pathology and Genetics. Tumours of the Digestive System. World Health Organization Classification of Tumours.* Lyon, France: IARC Press; 2000:237–240.
16. Maire F, Hammel P, Terris B, et al. Prognosis of malignant intraductal papillary mucinous tumours of the pancreas after surgical resection. Comparison with pancreatic ductal adenocarcinoma. *Gut.* 2002;51:717–722.
17. Minsky BD, Mies C, Rich TA, et al. Colloid carcinoma of the colon and rectum. *Cancer.* 1987;60:3103–3112.
18. Mizuta Y, Akazawa Y, Shiozawa K, et al. Pseudomyxoma peritonei accompanied by intraductal papillary mucinous neoplasm of the pancreas. *Pancreatology.* 2005;5:470–474.
19. Nakagohri T, Asano T, Kenmochi T, et al. Long-term surgical outcome of noninvasive and minimally invasive intraductal papillary mucinous adenocarcinoma of the pancreas. *World J Surg.* 2002;26:1166–1169.
20. Raimondo M, Tachibana I, Urrutia R, et al. Invasive cancer and survival of intraductal papillary mucinous tumors of the pancreas. *Am J Gastroenterol.* 2002;97:2553–2558.
21. Ronnett BM, Zahn CM, Kurman RJ, et al. A Clinicopathologic analysis of 109 cases with emphasis on distinguishing pathologic features, site of origin, prognosis, and relationship to "pseudomyxoma peritonei". *Am J Surg Pathol.* 1995;19:1390–1408.
22. Salvia R, Fernandez-del Castillo C, Bassi C, et al. Main-duct intraductal papillary mucinous neoplasms of the pancreas: clinical predictors of malignancy and long-term survival following resection. *Ann Surg.* 2004;239:677–678.
23. Shimada K, Sakamoto Y, Sano T, et al. Invasive carcinoma originating in an intraductal papillary mucinous neoplasm of the pancreas: a clinicopathologic comparison with a common type of invasive ductal carcinoma. *Pancreas.* 2006;32:281–287.
24. Sohn TA, Yeo CJ, Cameron JL, et al. Intraductal papillary mucinous neoplasms of the pancreas: an updated experience. *Ann Surg.* 2004;239:788–789.
25. Suzuki Y, Atomi Y, Sugiyama M. Cystic neoplasm of the pancreas: a Japanese multi-institutional study of intraductal papillary mucinous tumor and mucinous cystic tumor. *Pancreas.* 2004;28:241–246.
26. Wells M, Östör AG, Crum CP, et al. Epithelial tumours. In: Tavassoli FA, Devilee P, eds. *Pathology and Genetics of Tumours of the Breast and Female Genital Organs. World Health Organization Classification of Tumours.* Lyon, France: IARC Press; 2003: 262–269.
27. Yamao K, Ohashi K, Nakamura T, et al. The prognosis of intraductal papillary mucinous tumors of the pancreas. *Hepatogastroenterology.* 2000;47:1129–1134.

LINE-1 Hypomethylation Is Associated with Increased CpG Island Methylation in *Helicobacter pylori*–Related Enlarged-Fold Gastritis

Eiichiro Yamamoto,[1] Minoru Toyota,[1,2] Hiromu Suzuki,[1] Yutaka Kondo,[4] Tamana Sanomura,[5] Yoko Murayama,[6] Mutsumi Ohe-Toyota,[2] Reo Maruyama,[1] Masanori Nojima,[3] Masami Ashida,[2] Kyoko Fujii,[1] Yasushi Sasaki,[2] Norio Hayashi,[5] Mitsuru Mori,[3] Kohzoh Imai,[1] Takashi Tokino,[2] and Yasuhisa Shinomura[1]

[1]First Department of Internal Medicine; [2]Department of Molecular Biology, Cancer Research Institute; [3]Department of Public Health, Sapporo Medical University, Sapporo, Japan; [4]Division of Molecular Oncology, Aichi Cancer Center, Nagoya, Japan; [5]Department of Gastroenterology and Hepatology, Graduate School of Medicine, Osaka University, Suita, Japan; and [6]Department of Gastroenterology and Hepatology, Itami City Hospital, Itami, Japan

Abstract

Background: **The molecular mechanism by which *Helicobacter pylori* infection leads to gastric cancer is not fully understood. Similarly, patients with enlarged-fold (EF+) gastritis, one cause of which is *H. pylori* infection, have an increased risk for gastric cancer, although again molecular mechanism is unclear. In the present study, we analyzed the methylation status of long interspersed nucleotide elements (LINE-1) and three cancer-related genes in a panel of gastric mucosae, with or without EF+ gastritis.**

Methods: **We used bisulfite pyrosequencing to assess the levels of LINE-1, CDH1, CDH13, and PGP9.5 methylation in 78 gastric mucosa specimens from 48 patients.**

Results: **Levels of LINE-1 methylation were significantly reduced in mucosae from patients with EF+ gastritis. This hypomethylation of LINE-1 was associated with increased methylation of the 5′ CpG islands of the genes, which suggests that, in EF+ gastritis, the methylation of the promoter regions of certain genes is accompanied by global demethylation of repetitive sequences.**

Conclusions: **Our results indicate that genomewide hypomethylation and regional hypermethylation occur in EF+ gastritis and may contribute to the tumorigenesis of diffuse-type gastric cancers.** (Cancer Epidemiol Biomarkers Prev 2008;17(10):2555–64)

Introduction

Etiologic analysis has shown that infection by *Helicobacter pylori* plays a critical role in the development of gastric cancer, although the molecular mechanism is not fully understood (1). Moreover, most patients with *H. pylori*–related gastritis never develop a gastric malignancy. It would thus be highly desirable if one could identify molecular markers that were predictive of the risk for *H. pylori*–related gastric cancer. For instance, it is now widely accepted that intestinal-type gastric cancers arise from lesions containing intestinal metaplasia (2).

Enlarged gastric folds are associated with a variety of diseases, including hypertrophic gastritis, Ménétrier disease, Zollinger-Ellison syndrome, primary gastrin cell hyperplasia, gastric cancer, and lymphoma (3). *H. pylori* is a known cause of enlarged-fold (EF+) gastritis accompanied by foveolar hyperplasia, massive infiltration of inflammatory cells, and increased production of interleukin 1β and hepatocyte growth factor in the corpus mucosa (4-6). Notably, the mutagenicity of gastric juice in the body region of the stomach is significantly higher in the patients with *H. pylori*–related EF+ gastritis than in either *H. pylori*–negative (HP-) controls or *H. pylori*–positive (HP+) patients without enlarged fold (EF-; ref. 7). It has also been reported that the prevalence of diffuse-type gastric cancer in the gastric body region increases with increasing fold width (4). Taken together, these findings suggest that HP+/EF+ gastritis puts one at high risk of developing diffuse-type gastric cancer.

Epigenetic alterations play a key role in silencing genes in human tumors (8). In gastric cancer, for example, DNA methylation leads to the silencing of a variety of cancer-related genes involved in cell cycle regulation, apoptosis, immune function, cell signaling, and tumor invasion and metastasis (9-12). *H. pylori* infection reportedly induces methylation of various genes in the gastric mucosae, among which CDH1 is reportedly hypermethylated in HP+/EF+ gastritis (13). On the other hand, global levels of DNA methylation reportedly decline in various types of cancer (14-16). The role of global hypomethylation in cancer remains largely unexplored, although it is reportedly associated with

Received 2/4/08; revised 6/10/08; accepted 7/3/08.

Grant support: Grants-in-Aid for Scientific Research from the Ministry of Education, Culture, Sports, Science, and Technology (M. Toyota, K. Imai, T. Tokino, and Y. Shinomura), a Grant-in-Aid for the Third-term Cancer Control Strategy, and Grant-in-Aid for Cancer Research from the Ministry of Health, Labor, and Welfare, Japan (M. Toyota).

Requests for reprints: Yasuhisa Shinomura, First Department of Internal Medicine, Sapporo Medical University, South 1,West 16, Chuo-ku, Sapporo 060-8543, Japan. Phone: 81-11-611-2111, ext. 3211; Fax: 81-11-618-3313. E-mail: shinomura@sapmed.ac.jp

doi:10.1158/1055-9965.EPI-08-0112

Table 1. *H. pylori* infection, age, and sex of 48 patients

	H. pylori (−)	*H. pylori* (+), enlarged (−)	*H. pylori* (+), enlarged (+)
Age (y)	46.3 (23-78)	57.9 (22-81)	51.8 (38-63)
Age differences (SE) HP+/EF-	−12.7 (5.1), $P = 0.051$		
when compared with HP+/EF+	−5.5 (5.7), $P > 0.999$	7.2(4.8), $P = 0.431$	
Sex (male/female)	7/4	16/8	9/4

chromosomal instability. Moreover, global hypomethylation has been reported to correlate with hypermethylation of CpG islands (17), although other studies do not support this concept (16), and it remains unclear whether global hypomethylation and CpG island hypermethylation are two independent phenomena or are mechanistically linked.

Our aim in the present study was to begin to address these issues by using quantitative bisulfite pyrosequencing to examine the methylation of repetitive sequence long interspersed nucleotide elements (LINE-1) in a panel of gastric mucosae, with and without *H. pylori* infection. In addition, we analyzed the correlation between LINE-1 hypomethylation and the levels of CpG island methylation in patients with EF+ gastritis.

Materials and Methods

Patients and Specimens. In total, 78 specimens from 48 patients with gastritis were examined for methylation. These included 23 specimens of gastric mucosa from 13 patients who were HP+/EF+ (13), 37 specimens from 24 patients who were HP+/EF-, and 18 specimens from 11 patients who were HP- and served as controls. Average ages and sex ratios in the three groups are shown in Table 1. Written informed consent was obtained from every patient, and this study was approved by the institutional review board. In each case, the widths of the gastric body folds on double-contrast radiographs were measured using a computerized image analyzer. The diagnostic criteria for EF+ gastritis were *H. pylori* positivity and a maximum fold width in the gastric body >5 mm, which are consistent with earlier studies and the Sydney system (18). EF- patients were divided into two groups on the basis of the presence or absence of *H. pylori* infection, which was identified by histologic examination and by a rapid urease test (Pyloritek test, Serim Research Corp.). If either of these assays was positive, the patient was considered to be HP+. From each patient, gastric mucosa biopsy specimens were taken from the gastric body and antrum. DNA was prepared using a QIAamp DNA Mini Kit (Qiagen).

Bisulfite Treatment. Bisulfite treatment was carried out as described previously (19). Briefly, 2 μg of DNA was incubated with 10 mmol/L hydroquinone and 3 mol/L sodium bisulfite for 16 h at 37°C. The DNA was then purified using a PCR purification system (Promega). After precipitation with ethanol, the DNA was resuspended in 20 μL of distilled water and stored at -20°C until used.

Bisulfite Pyrosequencing. Pyrosequencing was carried out as described previously (14, 20). Bisulfite PCR primers were designed using PSQ Assay Design software (Biotage), and the primers and PCR conditions used for specific target genes are shown in Table 2. After PCR, the biotinylated PCR product was purified and made single stranded to act as a template in a pyrosequencing reaction run as recommended by the manufacturer (Biotage). The PCR products were bound to streptavidin-coated Sepharose beads, after which beads containing the immobilized PCR products were purified,

Table 2. Primer sequences used in this study

Pyrosequencing	Sequences	No. CpG sites analyzed
CDH13	F: 5′-GYGAGGTGTTTATTTYGTATTTGT-3′ R: 5′-AACCAACTTCCCAAATAAATCAAC-3′ Sequence: 5′-TGTTATGTAAAAYGAGGG-3′	2
CDH1		
Set1	F: 5′-TTTTTTGATTTTAGGTTTTAGTGAGTTAT-3′ R: 5′-TACCRACCACAACCAATCAACAAC-3′ Sequence: 5′-GATTTTAGGTTTTAGTGAGT-3′	3
Set2	F: 5′-GGAATTGTAAAGTATTTGTGAGTTTG-3′ R: 5′-RAAATACCTACAACAACAACAACAAC-3′ Sequence: 5′-GGAAGTTAGTTTAGATTTTA-3′	4
PGP9.5	F: 5′-AGTGAGATTGTAAGGTTTGGGGGTT-3′ R: 5′-ACCGCCCAAACTACAACTATAAAAC-3′ Sequence: 5′-GGGGTTYGTATTTATTTG-3′	4
LINE-1	F: 5′-TTTTGAGTTAGGTGTGGGATATA-3′ R: 5′-AAAATCAAAAAATTCCCTTTC-3′ Sequence: 5′-GGGTGGGAGTGAT-3′	3
Bisulfite sequencing		
CDH1	F: 5′-GGATTYGAATTTAGTGGAATTAGA-3′ R: 5′-CAAAACTAAAACRCRAAACTTAC-3′	38

NOTE: Y = C or T, R = A or G.

washed, and denatured using a 0.2 mol/L NaOH solution. Thereafter, 0.3 μmol/L pyrosequencing primers were annealed to the purified single-stranded PCR product, and pyrosequencing was carried out using a PSQ HS 96 Pyrosequencing System (Biotage), after which methylation was then quantified using PSQ Assay Design software (Biotage).

Bisulfite Sequencing. To amplify the CDH1 promoter region, PCR was carried out using primers that amplify the region around the transcription start site of the gene (Fig. 1B, Table 2). The resultant PCR products were then cloned into pCR4.0 vector using a TOPO-TA Cloning Kit (Invitrogen). The sequencing reaction was carried out using a BigDye terminator cycle sequencing kit (PE Biosystems), and sequencing was done using an ABI PRISM 3100 sequencer according to the manufacturer guidelines (Applied Biosystems). Alleles that showed methylation of >80% of their CpG sites were considered to be densely methylated.

Statistical Analysis. Proportions and mean values between two groups were compared using Fisher's exact test (two tailed) or Student's *t* test. Methylation levels and densities among three groups were compared using one-way ANOVA with Games-Howell post hoc test and age-adjusted analysis of covariance (ANCOVA) with Bonferroni Correction for multiple comparisons. Pearson's correlation coefficients were calculated between methylation levels of each gene and by each method. $P < 0.05$ was considered statistically significant. All statistical analyses were carried out using Statistical Package for the Social Sciences software 15.0 J (SPSS, Inc.).

Results

Hypomethylation of LINE-1 in EF+ Gastritis. We initially used pyrosequencing to assess the levels of LINE-1 methylation in a panel of gastric mucosae (Figs. 1 and 2, Table 3). Among 48 patients, 13 patients were

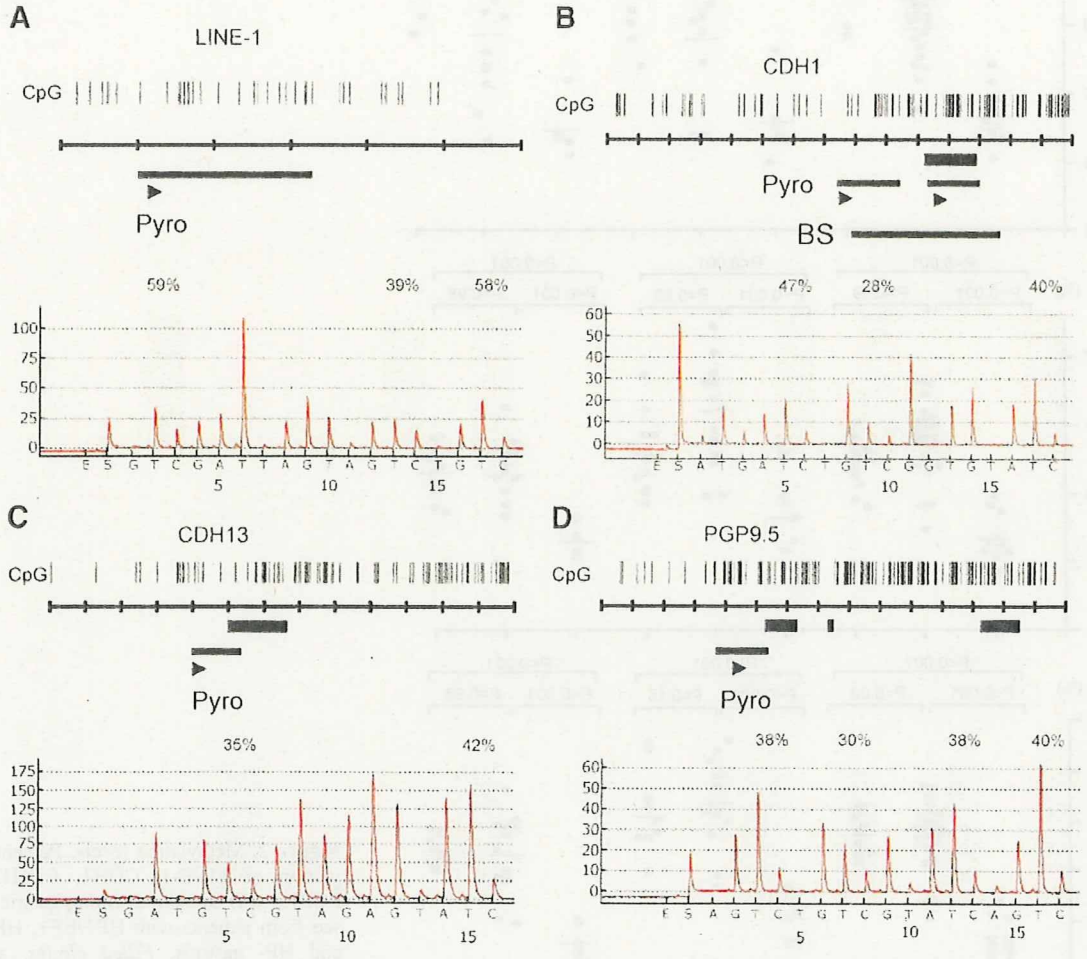

Figure 1. Quantitative pyrosequencing analysis of LINE-1 (**A**), CDH1 (**B**), CDH13 (**C**), and PGP9.5 (**D**) methylation. *Top,* schematic representation of the CpG islands analyzed; *horizontal bars,* regions analyzed by pyrosequencing (*Pyro*) and bisulfite sequencing (*BS*); *bent bars,* transcription start sites; *bottom,* representative pyrograms; *gray columns,* regions of C-to-T polymorphic sites. Percent methylation is shown above the peak. *Y-axis,* signal peaks reflecting to the number of nucleotides incorporated; *X-axis,* nucleotides incorporated.

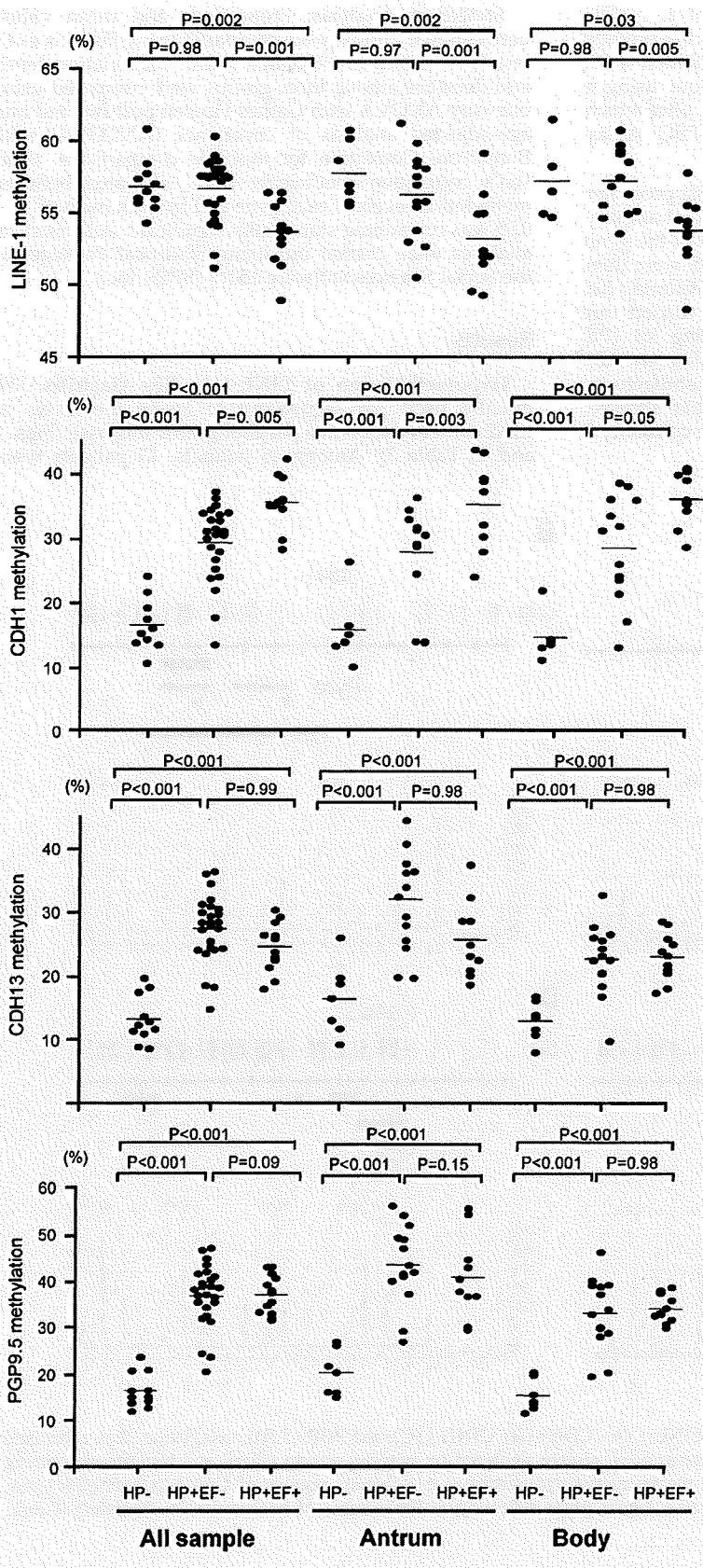

Figure 2. Methylation levels. Percent methylation of LINE-1, CDH1, CDH13, and PGP9.5 was compared among gastric mucosae from patients with HP+/EF+, HP+/EF-, and HP- gastritis. *Filled circles,* average methylation of multiple CpG sites. In 30 cases, specimens were obtained from the antrum and body, and the average methylation levels are shown. Genes analyzed are shown on the left. *Horizontal bars,* average methylation levels in total cases.

Table 3. Summary of pyrosequence results

All subjects				Antrum				Body			
Gene	HP/EF status	*n* (mean ± SD)	95% CI	Gene	HP/EF status	*n* (mean ± SD)	95% CI	Gene	HP/EF status	*n* (mean ± SD)	95% CI
LINE-1	HP−	11 (56.8 ± 1.8)	55.6-57.9	*LINE-1*	HP−	7 (57.7 ± 2.1)	55.7-59.6	*LINE-1*	HP−	7 (57.2 ± 2.3)	55.0-59.3
	HP+/EF−	24 (56.7 ± 2.2)	55.7-57.6		HP+/EF−	13 (56.2 ± 3.1)	54.2-58.0		HP+/EF−	13 (57.4 ± 2.3)	56.0-58.7
	HP+/EF+	13 (53.6 ± 2.1)	52.3-54.9		HP+/EF+	10 (53.2 ± 3.1)	50.9-55.4		HP+/EF+	10 (53.8 ± 2.5)	51.9-55.5
CDH1	HP−	10 (16.4 ± 4.1)	13.4-19.2	*CDH1*	HP−	6 (15.6 ± 5.6)	9.74-21.4	*CDH1*	HP−	6 (14.4 ± 3.7)	10.5-18.3
	HP+/EF−	23 (29.8 ± 4.9)	27.6-31.9		HP+/EF−	12 (28.9 ± 5.9)	25.1-32.6		HP+/EF−	12 (29.6 ± 7.1)	25.0-34.1
	HP+/EF+	12 (35.3 ± 4.2)	32.6-37.9		HP+/EF+	9 (35.0 ± 7.0)	29.6-40.3		HP+/EF+	9 (35.9 ± 4.3)	32.6-39.2
CDH13	HP−	11 (16.4 ± 3.7)	13.8-18.8	*CDH13*	HP−	7 (20.2 ± 4.9)	15.6-24.7	*CDH13*	HP−	7 (15.3 ± 3.4)	12.1-18.4
	HP+/EF−	24 (37.2 ± 6.3)	34.5-39.8		HP+/EF−	13 (44.5 ± 7.4)	40.0-49.0		HP+/EF−	13 (34.0 ± 6.9)	29.8-38.1
	HP+/EF+	13 (36.9 ± 4.1)	34.4-39.4		HP+/EF+	10 (40.7 ± 8.8)	34.3-46.9		HP+/EF+	10 (33.6 ± 2.9)	31.5-35.6
PGP9.5	HP−	11 (13.2 ± 3.7)	10.6-15.6	*PGP9.5*	HP−	7 (16.3 ± 5.7)	11.0-21.5	*PGP9.5*	HP−	7 (12.9 ± 3.1)	10.0-15.7
	HP+/EF−	24 (27.7 ± 5.0)	25.6-29.8		HP+/EF−	13 (32.9 ± 7.3)	28.5-37.3		HP+/EF−	13 (23.0 ± 5.4)	19.7-26.3
	HP+/EF+	13 (24.5 ± 3.8)	22.2-26.8		HP+/EF+	10 (25.6 ± 6.0)	21.3-29.9		HP+/EF+	10 (22.7 ± 3.8)	19.9-25.3

HP+/EF+, 24 patients were HP+/EF-, and 11 patients were HP-. We found that the average levels of LINE-1 methylation were similar in specimens from patients with HP+/EF- and HP- gastritis (56.7% and 56.8%; 95% CI, 55.7-57.6 and 55.6-57.9, respectively; $P = 0.98$). On the other hand, specimens from patients with HP+/EF+ gastritis showed significantly lower levels of LINE-1 methylation (53.6%; 95% CI, 52.3-54.9) than either of the other two groups (HP- versus HP+/EF+ 95% CI, 1.2-5.2; $P = 0.002$; HP+/EF- versus HP+/EF+ 95% CI, 1.2-4.9; $P = 0.001$). Because there were age differences between HP+/EF+ and other two groups, we did age-adjusted ANCOVA with Bonferroni Correction for multiple comparisons. We found the same tendency for the differences by age-adjusted model, indicating that age-related differences in methylation did not account for the results (Table 4).

In 30 patients, specimens were obtained from the gastric antrum and body, which enabled us to compare the levels of LINE-1 methylation in these two areas. We found that in HP+/EF+ cases, methylation of LINE-1 in the gastric body was significantly lower than that in either HP+/EF- (53.8% versus 57.4%; $P = 0.005$) or HP- cases (53.8% versus 57.2%; $P = 0.03$). Likewise, methylation of LINE-1 in the antrum in HP+/EF+ cases was significantly lower than that in HP+/EF- (53.2% versus 56.2%; $P = 0.001$) or HP- cases (53.2% versus 57.7%; $P = 0.002$). There was a significant correlation between the methylation levels of LINE-1 in the antrum and body ($R = 0.58$; $P = 0.001$; Table 5).

Table 4. The difference of mean age-adjusted levels of *LINE-1, CDH1, CDH13, and PGP9.5* methylation

Gene	HP/EF status	compared with	difference	SE	*P*	95% CI
LINE-1	HP−	HP+/EF−	0.3	0.8	>0.999	(−1.8 to 2.3)
		HP+/EF+	3.2	0.9	0.002	(1.0 to 5.4)
	HP+/EF−	HP+/EF+	3.0	0.7	0.001	(1.0 to 4.8)
CDH1	HP−	HP+/EF−	−13.4	1.8	<0.001	(−18.0 to −8.8)
		HP+/EF+	−19.5	2.1	<0.001	(−24.8 to −14.1)
	HP+/EF−	HP+/EF+	−6.0	1.8	0.006	(−10.5 to −1.4)
CDH13	HP−	HP+/EF−	−18.2	1.7	<0.001	(−22.4 to −13.9)
		HP+/EF+	−18.4	1.9	<0.001	(−23.0 to −13.7)
	HP+/EF−	HP+/EF+	−1.2	1.6	>0.999	(−5.2 to 2.7)
PGP9.5	HP−	HP+/EF−	−12.3	1.4	<0.001	(−15.8 to −8.7)
		HP+/EF+	−10.4	1.5	<0.001	(−14.1 to −6.5)
	HP+/EF−	HP+/EF+	1.9	1.3	0.442	(−1.3 to 5.1)

Table 5. Correlation of methylation levels in antrum and body

	Mean (SD)		Correlation coefficient (R =)	P
	Antrum	Body		
LINE-1	55.5 (3.3)	56.2 (2.9)	0.58	0.001
CDH1	28.0 (9.4)	28.3 (9.6)	0.82	<0.001
CDH13	37.6 (12.2)	29.5 (9.4)	0.71	<0.001
PGP9.5	26.6 (9.1)	20.5 (6.0)	0.67	<0.001

Hypermethylation of 5′ CpG Islands of Genes Is Associated with Hypomethylation of LINE-1 in EF+ Gastritis. To examine the methylation levels of the 5′ CpG islands of genes involved in HP+/EF+ gastritis, we used pyrosequencing to assess methylation of CDH1, CDH13, and PGP9.5 (Fig. 1). For all three genes, the level of methylation was significantly higher in specimens from patients with *H. pylori* infection (Fig. 2; Table 3). Furthermore, methylation of CDH1 was significantly higher in HP+/EF+ cases (35.3%) than in either HP+/EF- (29.8%) or HP- (16.4%) cases (P < 0.001; P = 0.005). Methylation of CDH13 and PGP9.5 was higher in HP+/EF+ cases (CDH13, 36.9%; PGP9.5, 24.5%) than in HP-/EF- cases (CDH13, 16.4%; P < 0.001; PGP9.5, 13.2%; P < 0.001) but was similar to that in HP+/EF- cases (CDH13, 37.2%; P = 0.99; PGP9.5, 27.7%; P = 0.09). Regression analysis of the levels of methylation of all three genes revealed significant correlations between the methylation of CDH1 and CDH13, CDH1 and PGP9.5, and CDH13 and PGP9.5 (Fig. 3A). Overall, there was a significant correlation between the levels of methylation in the antrum and body (CDH1, R = 0.82; P < 0.001; CDH13, R = 0.71; P < 0.001; PGP9.5, R = 0.67; P < 0.001; Table 5).

We next examined the correlation between levels of LINE-1 methylation and methylation of the CDH1, CDH13, and PGP9.5 CpG islands (Fig. 3B), and observed inverse relations between the level of LINE-1 methylation and methylation of CDH1 (R = -0.40; P = 0.0003), CDH13 (R = -0.31; P = 0.005), and PGP9.5 (R = -0.23; P = 0.04).

Because the median value of LINE-1 methylation was 56.0%, we used that as a cut point to separate specimens with hypomethylation of LINE-1 (<56%) from those without it (LINE-1>56%). We found that hypomethylation of LINE-1 was significantly associated with EF+ gastritis (P = 0.008) and methylation of CDH1 (P = 0.05; Table 1).

Dense Methylation of CDH1 in EF+ Gastritis. With pyrosequencing, we examined only seven CpG sites in the CDH1 promoter. For that reason, we also investigated the density of CDH1 methylation by bisulfite-sequencing PCR products amplified using primers that contained the region around the transcription start site of the gene (Fig. 4A and B). Gastric mucosae from HP+/EF- cases showed increased methylation of CDH1, but the density of CDH1 methylation was higher in HP+/EF+ cases (n = 8; average, 27.8%) than in either HP- (n = 8; average, 3.3%) or HP+/EF- cases (n = 17; average, 15.6%). When we then determined the percentages of clones that showed >80% methylation of CpG sites, we found that, in the antrum, the percentages were higher in HP+/EF+ cases (average, 11.6%) than in HP- (average, 0%) and HP+/EF- (average, 9.6%) cases, although the difference between the two HP+ groups was not significant (Fig. 1A). In the gastric body too, the percentages of clones showing methylation of >80% of CpG sites were higher in HP+/EF+ cases (average, 9.5%) than in the other two groups (average, 0% and 3.7%, respectively;

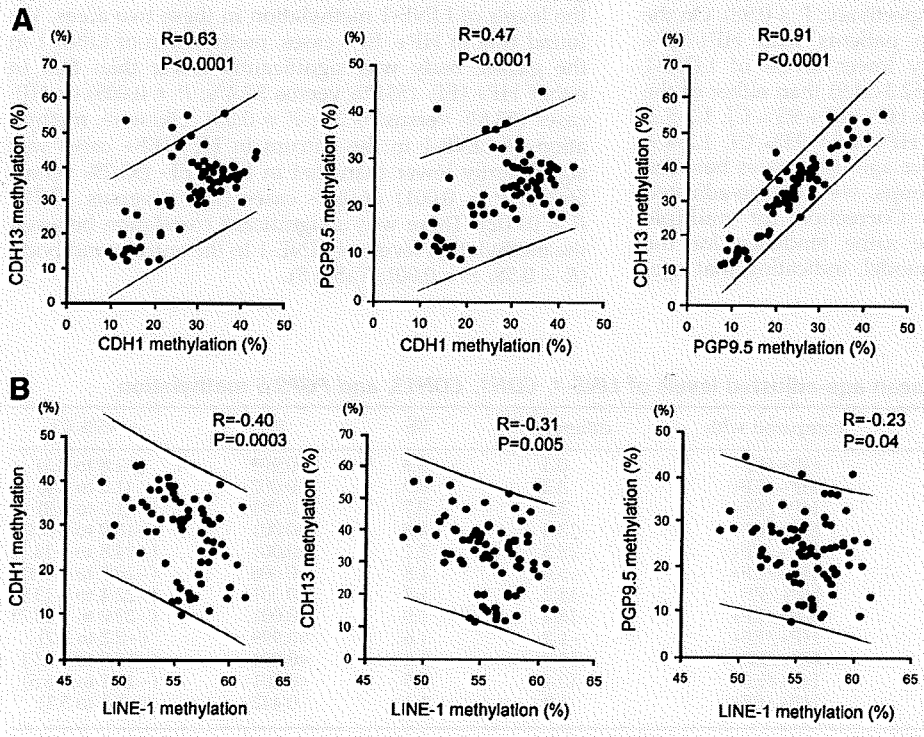

Figure 3. Correlation of methylation among genes. **A.** Regression analysis showing concordance of the methylation of CDH1, CDH13, and PGP9.5 in gastric mucosae. *Solid lines*, 95% CI. **B.** Inverse relation between LINE-1 methylation and CpG island methylation.

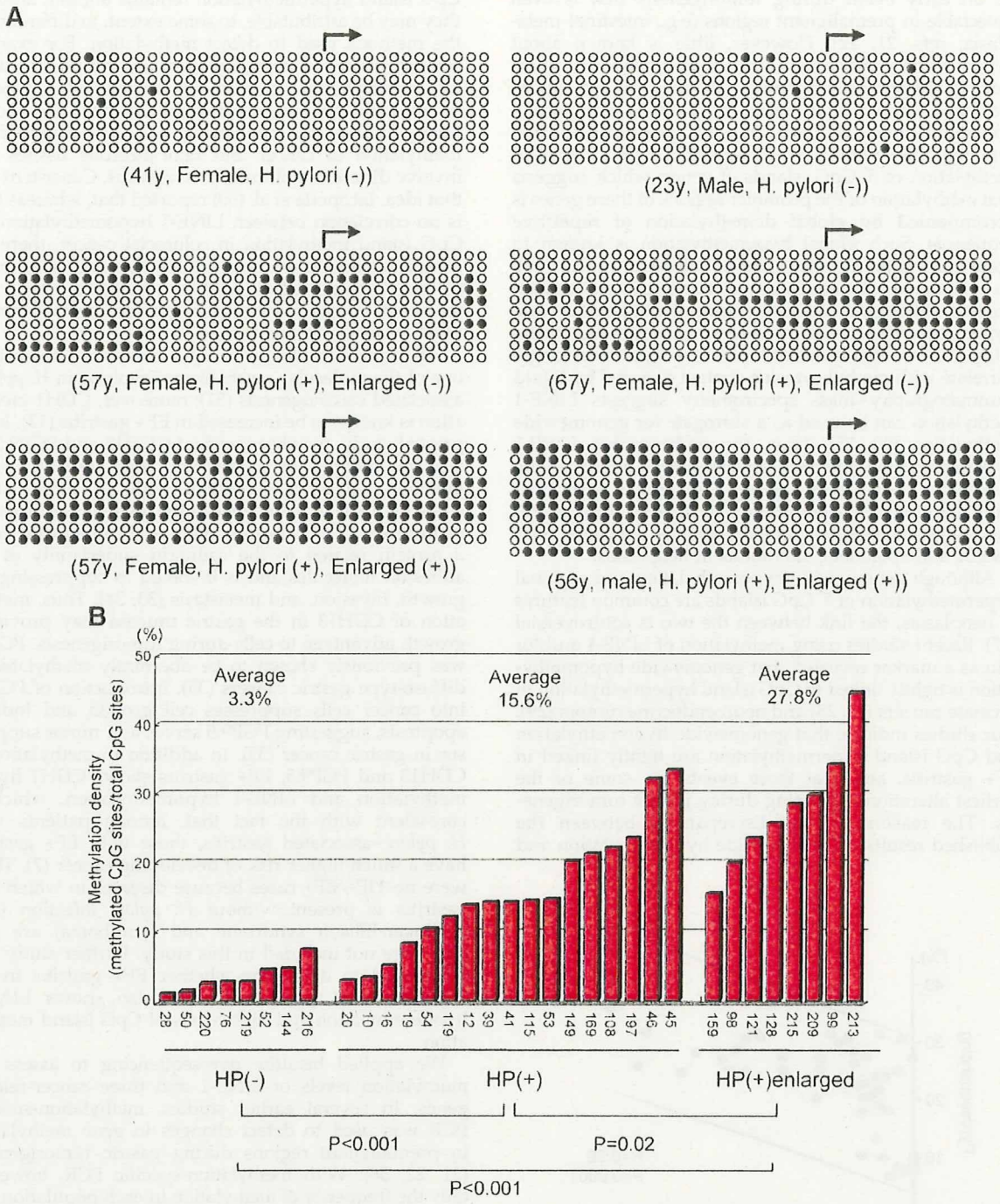

Figure 4. A. Bisulfite sequencing of CDH1 in HP+/EF+ gastritis. *Vertical columns,* CpG sites; *horizontal arrows,* transcription start sites; *open circles,* unmethylated CpG sites; *filled circles,* methylated CpG sites. The cases examined are below the columns. **B.** Density of CDH1 methylation in gastric mucosae; CpG site methylation is expressed as a percentage of the total (*Y-axis*). Average of density of methylation in HP+/EF+ gastritis is higher than in HP+/EF- and HP- gastritis.

Fig. 1B). Note that there was a good correlation between the methylation levels detected by pyrosequencing and those detected by bisulfite sequencing (R = 0.59; P < 0.0001; Fig. 5).

Discussion

DNA methylation plays a key role in the silencing of genes in cancer (8). Indeed, DNA methylation seems to

be an early event during tumorigenesis that is even detectable in premalignant regions (e.g., intestinal metaplasia; refs. 21, 22). However, little is known about genomewide methylation status in premalignant regions during gastric tumorigenesis. In the present study, we have shown that levels of LINE-1 methylation are significantly reduced in EF+ gastritis and that this hypomethylation was associated with increased methylation of 5′ CpG islands of genes, which suggests that methylation of the promoter regions of these genes is accompanied by global demethylation of repetitive sequences. Such global hypomethylation is known to occur during the development of colorectal cancer (15). Its functional consequences in tumorigenesis remain unclear, although it has been proposed that genomewide hypomethylation gives increase to chromosomal instability (23, 24). That levels of LINE-1 methylation strongly correlate with methyl cytosine content detected by liquid chromatography–mass spectrometry suggests LINE-1 methylation can be used as a surrogate for genomewide methylation (20, 25). Thus, the findings that LINE-1 hypomethylation inversely correlates with microsatellite instability in colorectal cancers (14) and is associated with alteration of chromosome 8 in prostate cancers (26) suggest genomewide hypomethylation is associated with genetic and epigenetic alterations in neoplasias.

Although genomewide hypomethylation and regional hypermethylation of 5′ CpG islands are common features of neoplasias, the link between the two is controversial (27). Recent studies using methylation of LINE-1 and/or Alu as a marker revealed that genomewide hypomethylation is tightly linked to CpG island hypermethylation in prostate cancers (17, 28) and neuroendocrine tumors (29). Our studies indicate that genomewide hypomethylation and CpG island hypermethylation are tightly linked in EF+ gastritis, and that these events are some of the earliest alterations occurring during gastric tumorigenesis. The reason for the discrepancies between the published results on genomewide hypomethylation and CpG island hypermethylation remains unclear, although they may be attributable, to some extent, to differences in the methods used to detect methylation. For example, several studies used methylation-specific PCR to detect hypermethylation of promoter regions (16), whereas others used quantitative methylation analyses such as MethyLight or Pyrosequencing (14, 30). Alternatively, methylation in cancer and noncancerous tissues may involve different molecular mechanisms. Consistent with that idea, Iacopetta et al. (30) reported that, whereas there is no correlation between LINE-1 hypomethylation and CpG island methylation in colorectal cancer, there is a significant correlation between the two events in normal colon. Further studies will be needed to clarify the molecular mechanisms responsible for aberrant methylation in noncancerous tissues.

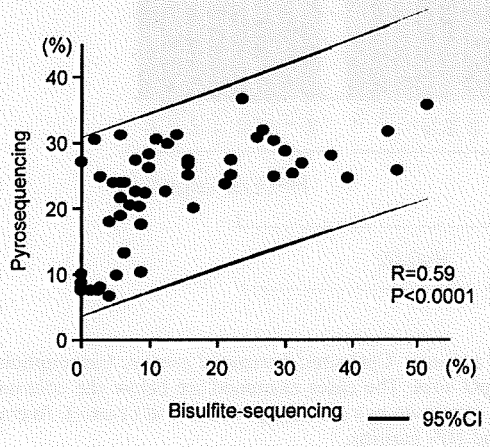

Figure 5. Regression analysis of methylation levels detected using pyrosequencing and bisulfite sequencing. Levels of CDH1 methylation detected by pyrosequencing are plotted against the density of CDH1 methylation detected by bisulfite sequencing.

Aberrant methylation of CpG islands is known to be one of the molecular mechanisms involved in *H. pylori*–associated carcinogenesis (31); moreover, CDH1 methylation is known to be increased in EF+ gastritis (13). In the present study, we observed that CDH13 and PGP9.5 are also methylated in gastric mucosae with *H. pylori* infection, which is consistent with an earlier study showing CDH13 to be aberrantly methylated in gastric cancer (32). CDH13 (also known as H-cadherin) encodes a protein related to the cadherin superfamily of cell adhesion molecules and is involved in suppressing cell growth, invasion, and metastasis (33, 34). Thus, methylation of CDH13 in the gastric mucosa may provide a growth advantage to cells during tumorigenesis. PGP9.5 was previously shown to be aberrantly methylated in diffuse-type gastric cancers (35). Introduction of PGP9.5 into cancer cells suppresses cell growth and induces apoptosis, suggesting PGP9.5 serves as a tumor suppressor in gastric cancer (35). In addition to methylation of CDH13 and PGP9.5, EF+ gastritis shows CDH1 hypermethylation and LINE-1 hypomethylation, which is consistent with the fact that, among patients with *H. pylori*–associated gastritis, those with EF+ gastritis have a much higher risk of developing cancer (7). There were no HP-/EF+ cases because diseases in which EF+ gastritis is present without *H. pylori* infection (e.g., Zollinger-Ellison syndrome and lymphoma) are rare and were not included in this study. Further study will be needed to determine whether EF+ gastritis in the absence of *H. pylori* infection also shows LINE-1 hypomethylation and high levels of CpG island methylation.

We applied bisulfite pyrosequencing to assess the methylation levels of LINE-1 and three cancer-related genes. In several earlier studies, methylation-specific PCR was used to detect changes in gene methylation in premalignant regions during gastric tumorigenesis (21, 22, 36). With methylation-specific PCR, however, only the frequency of methylation in each population can be analyzed. Bisulfite pyrosequencing offers a semiquantitative, high throughput, and reliable method that has an inbuilt internal control for adequacy of bisulfite treatment (37). This approach enabled us to determined that levels of CDH1, CDH13, and PGP9.5 methylation are positively correlated, and that there is an inverse relation between LINE-1 and CpG island methylation.

The molecular mechanism underlying genomewide hypomethylation in EF+ gastritis remains unknown; however, our finding that methylation levels in the

Table 6. Characteristics of gastritis with or without *LINE-1* hypomethylation

	LINE-1<56%	*LINE-1*>56%	*P*
	(*n* = 24)	(*n* = 24)	
Sex			
Male	12	19	0.07
Female	12	5	
Age			
Mean (SD)	52.7 (12.6)	54.5 (15.1)	0.85
H. pylori			
Positive	19	18	1
Negative	5	6	
Enlarged fold			
Positive	11	2	0.008
Negative	13	22	
Methylation			
CDH1	32.2 (7.7)	24.2 (8.2)	0.054
CDH13	36.0 (10.4)	29.4 (11.4)	0.312
PGP9.5	25.3 (7.8)	21.7 (8.3)	0.742

antrum and body correlate with one another suggests that it is the degree of inflammation that affects DNA methylation in both the pyloric and fundic glands from different parts of stomach. Recent studies suggest a role for proteins involved in the maintenance of heterochromatin in the silencing of repetitive elements (38). For example, Lsh deficiency leads to abnormal heterochromatin organization, with a genomewide loss of DNA methylation (39). Moreover, histone H3 lysine-27 demethylase Jmjd3 is induced by inflammation and is involved in altered histone modification in inflamed tissues (40). This suggests that altered chromatin structure and/or histone modification induced by inflammation may be involved in global demethylation, although that idea remains to be tested. Nevertheless, hypomethylation of LINE-1 may represent a much needed molecular marker with which to predict the risk for gastric cancer associated with EF+ gastritis.

In conclusion, we have shown that LINE-1 hypomethylation is significantly associated with CpG island hypermethylation in EF+ gastritis. Our results not only shed light on the pathogenesis of gastric cancer associated with *H. pylori* infection, but also suggest that hypermethylation of gene promoters is often associated with global demethylation of repetitive sequences during tumorigenesis Table 6.

Disclosure of Potential Conflicts of Interest

No potential conflicts of interest were disclosed.

Acknowledgments

The costs of publication of this article were defrayed in part by the payment of page charges. This article must therefore be hereby marked *advertisement* in accordance with 18 U.S.C. Section 1734 solely to indicate this fact.

We thank Dr. William F. Goldman for editing the manuscript.

References

1. Uemura N, Okamoto S, Yamamoto S, et al. *Helicobacter pylori* infection and the development of gastric cancer. N Engl J Med 2001;345:784–9.
2. Correa P, Houghton J. Carcinogenesis of *Helicobacter pylori*. Gastroenterology 2007;133:659–72.
3. Komorowski RA, Caya JG. Hyperplastic gastropathy. Clinicopathologic correlation. Am J Surg Pathol 1991;15:577–85.
4. Murayama Y, Miyagawa J, Shinomura Y, et al. Morphological and functional restoration of parietal cells in *Helicobacter pylori* associated enlarged fold gastritis after eradication. Gut 1999;45:653–61.
5. Yasunaga Y, Shinomura Y, Kanayama S, et al. Mucosal interleukin-1 β production and acid secretion in enlarged fold gastritis. Aliment Pharmacol Ther 1997;11:801–9.
6. Yasunaga Y, Shinomura Y, Kanayama S, et al. Improved fold width and increased acid secretion after eradication of the organism in *Helicobacter pylori* associated enlarged fold gastritis. Gut 1994;35:1571–4.
7. Nishibayashi H, Kanayama S, Kiyohara T, et al. *Helicobacter pylori*-induced enlarged-fold gastritis is associated with increased mutagenicity of gastric juice, increased oxidative DNA damage, and an increased risk of gastric carcinoma. J Gastroenterol Hepatol 2003;18:1384–91.
8. Jones PA, Baylin SB. The epigenomics of cancer. Cell 2007;128:683–92.
9. Satoh A, Toyota M, Ikeda H, et al. Epigenetic inactivation of class II transactivator (CIITA) is associated with the absence of interferon-γ-induced HLA-DR expression in colorectal and gastric cancer cells. Oncogene 2004;23:8876–86.
10. Satoh A, Toyota M, Itoh F, et al. DNA methylation and histone deacetylation associated with silencing DAP kinase gene expression in colorectal and gastric cancers. Br J Cancer 2002;86:1817–23.
11. Satoh A, Toyota M, Itoh F, et al. Epigenetic inactivation of CHFR and sensitivity to microtubule inhibitors in gastric cancer. Cancer Res 2003;63:8606–13.
12. Suzuki H, Itoh F, Toyota M, et al. Inactivation of the 14-3-3 σ gene is associated with 5′ CpG island hypermethylation in human cancers. Cancer Res 2000;60:4353–7.
13. Miyazaki T, Murayama Y, Shinomura Y, et al. E-cadherin gene promoter hypermethylation in *H. pylori*-induced enlarged fold gastritis. Helicobacter 2007;12:523–31.
14. Estecio MR, Gharibyan V, Shen L, et al. LINE-1 hypomethylation in cancer is highly variable and inversely correlated with microsatellite instability. PLoS ONE 2007;2:e399.
15. Feinberg AP, Vogelstein B. Hypomethylation distinguishes genes of some human cancers from their normal counterparts. Nature 1983;301:89–92.
16. Kaneda A, Tsukamoto T, Takamura-Enya T, et al. Frequent hypomethylation in multiple promoter CpG islands is associated with global hypomethylation, but not with frequent promoter hypermethylation. Cancer Sci 2004;95:58–64.
17. Cho NY, Kim BH, Choi M, et al. Hypermethylation of CpG island loci and hypomethylation of LINE-1 and Alu repeats in prostate adenocarcinoma and their relationship to clinicopathological features. J Pathol 2007;211:269–77.
18. Dixon MF, Genta RM, Yardley JH, Correa P. Classification and grading of gastritis. The updated Sydney System. International Workshop on the Histopathology of Gastritis, Houston 1994. Am J Surg Pathol 1996;20:1161–81.
19. Clark SJ, Harrison J, Paul CL, Frommer M. High sensitivity mapping of methylated cytosines. Nucleic Acids Res 1994;22:2990–7.
20. Yang AS, Estecio MR, Doshi K, et al. A simple method for estimating global DNA methylation using bisulfite PCR of repetitive DNA elements. Nucleic Acids Res 2004;32:e38.
21. Kang GH, Shim YH, Jung HY, et al. CpG island methylation in premalignant stages of gastric carcinoma. Cancer Res 2001;61:2847–51.
22. Lee JH, Park SJ, Abraham SC, et al. Frequent CpG island methylation in precursor lesions and early gastric adenocarcinomas. Oncogene 2004;23:4646–54.
23. Gaudet F, Hodgson JG, Eden A, et al. Induction of tumors in mice by genomic hypomethylation. Science 2003;300:489–92.
24. Karpf AR, Matsui S. Genetic disruption of cytosine DNA methyltransferase enzymes induces chromosomal instability in human cancer cells. Cancer Res 2005;65:8635–9.
25. Yang AS, Doshi KD, Choi SW, et al. DNA methylation changes after 5-aza-2′-deoxycytidine therapy in patients with leukemia. Cancer Res 2006;66:5495–503.
26. Schulz WA, Elo JP, Florl AR, et al. Genomewide DNA hypomethylation is associated with alterations on chromosome 8 in prostate carcinoma. Genes Chromosomes Cancer 2002;35:58–65.
27. Ehrlich M, Woods CB, Yu MC, et al. Quantitative analysis of associations between DNA hypermethylation, hypomethylation, and DNMT RNA levels in ovarian tumors. Oncogene 2006;25:2636–45.

28. Florl AR, Steinhoff C, Muller M, et al. Coordinate hypermethylation at specific genes in prostate carcinoma precedes LINE-1 hypomethylation. Br J Cancer 2004;91:985–94.
29. Choi IS, Estecio MR, Nagano Y, et al. Hypomethylation of LINE-1 and Alu in well-differentiated neuroendocrine tumors (pancreatic endocrine tumors and carcinoid tumors). Mod Pathol 2007;20: 802–10.
30. Iacopetta B, Grieu F, Phillips M, et al. Methylation levels of LINE-1 repeats and CpG island loci are inversely related in normal colonic mucosa. Cancer Sci 2007;98:1454–60.
31. Maekita T, Nakazawa K, Mihara M, et al. High levels of aberrant DNA methylation in *Helicobacter pylori*-infected gastric mucosae and its possible association with gastric cancer risk. Clin Cancer Res 2006; 12:989–95.
32. Hibi K, Kodera Y, Ito K, Akiyama S, Nakao A. Methylation pattern of CDH13 gene in digestive tract cancers. Br J Cancer 2004;91:1139–42.
33. Lee SW. H-cadherin, a novel cadherin with growth inhibitory functions and diminished expression in human breast cancer. Nat Med 1996;2:776–82.
34. Lee SW, Reimer CL, Campbell DB, et al. H-cadherin expression inhibits *in vitro* invasiveness and tumor formation *in vivo*. Carcinogenesis 1998;19:1157–9.
35. Yamashita K, Park HL, Kim MS, et al. PGP9.5 methylation in diffuse-type gastric cancer. Cancer Res 2006;66:3921–7.
36. Perri F, Cotugno R, Piepoli A, et al. Aberrant DNA methylation in non-neoplastic gastric mucosa of *H. pylori* infected patients and effect of eradication. Am J Gastroenterol 2007;102:1361–71.
37. Colella S, Shen L, Baggerly KA, Issa JP, Krahe R. Sensitive and quantitative universal pyrosequencing methylation analysis of CpG sites. Biotechniques 2003;35:146–50.
38. Muegge K. Lsh, a guardian of heterochromatin at repeat elements. Biochem Cell Biol 2005;83:548–54.
39. Dennis K, Fan T, Geiman T, Yan Q, Muegge K. Lsh, a member of the SNF2 family, is required for genome-wide methylation. Genes Dev 2001;15:2940–4.
40. De Santa F, Totaro MG, Prosperini E, et al. The histone H3 lysine-27 demethylase Jmjd3 links inflammation to inhibition of polycomb-mediated gene silencing. Cell 2007;130:1083–94.

Carcinogenesis vol.29 no.7 pp.1312–1318, 2008
doi:10.1093/carcin/bgn060
Advance Access publication February 29, 2008

Cytoplasmic RASSF2A is a proapoptotic mediator whose expression is epigenetically silenced in gastric cancer

Reo Maruyama[1,2,†], Kimishige Akino[1,2,†], Minoru Toyota[1,2,*], Hiromu Suzuki[1], Takashi Imai[2,3], Mutsumi Ohe-Toyota[2], Eiichiro Yamamoto[1], Masanori Nojima[4], Tomoko Fujikane[2,5], Yasushi Sasaki[2], Toshiharu Yamashita[6], Yoshiyuki Watanabe[2,7], Hiroyoshi Hiratsuka[3], Koichi Hirata[5], Fumio Itoh[7], Kohzoh Imai[1], Yasuhisa Shinomura[1] and Takashi Tokino[2]

[1]First Department of Internal Medicine, [2]Department of Molecular Biology, Cancer Research Institute, [3]Department of Oral Surgery, [4]Department of Public Health, [5]First Department of Surgery and [6]Department of Dermatology, Sapporo Medical University, Sapporo 060-8556, Japan and [7]Department of Gastroenterology and Hepatology, Saint Marianna University, School of Medicine, Kawasaki 216-8511, Japan

*To whom correspondence should be addressed. Tel: +81 11 611 2111 ext. 3210; Fax: +81 11 611 2282;
Email: mtoyota@sapmed.ac.jp
Correspondence may also be addressed to Yasuhisa Shinomura.
Email: shinomura@sapmed.ac.jp

Gastric cancer cells often show altered Ras signaling, though the underlying molecular mechanism is not fully understood. We examined the expression profile of eight ras-association domain family (*RASSF*) genes plus MST1/2 and found that *RASSF2A* is the most frequently downregulated in gastric cancer. *RASSF2A* was completely silenced in 6 of 10 gastric cancer cell lines as a result of promoter methylation, and expression was restored by treating the cells with 5-aza-2′-deoxycytidine. Introduction of RASSF2A into non-expressing cell lines suppressed colony formation and induced apoptosis. These effects were associated with the cytoplasmic localization of RASSF2A and morphological changes to the cells. Complementary DNA microarray analysis revealed that RASSF2A suppresses the expression of inflammatory cytokines, which may in turn suppress angiogenesis and invasion. In primary gastric cancers, aberrant methylation of *RASSF2A* was detected in 23 of 78 (29.5%) cases, and methylation correlated significantly with an absence of the lymphatic invasion, absence of venous invasion, absence of lymph node metastasis, less advanced stages, Epstein–Barr virus, absence of p53 mutations and the presence of the CpG island methylator phenotype-high. These results suggest that epigenetic inactivation of *RASSF2A* is required for tumorigenesis in a subset of gastric cancers.

Introduction

Gastric cancer is one of the most common of human neoplasias (1). It often arises through the accumulation of multiple genetic changes, including mutation of *APC*, *K-ras* and *p53*, but the frequencies of oncogene and tumor suppressor gene mutation in gastric cancer are relatively low, as compared those seen in colorectal cancer (2,3). On the other hand, recent studies have shown that epigenetic alterations (e.g. DNA methylation) play a key role in silencing such cancer-related genes such as *p16INK4A*, *CHFR*, *E-cadherin*, *14-3-3σ* and *DAP-kinase* (4–7), and genome-wide methylation screening has identified a number of genes inactivated by DNA methylation in gastric cancer (8,9). In that regard, *Helicobacter pylori* infection, a potent gastric carcinogenic factor, reportedly induces methylation of various genes in the gastric mucosa (10). Still, the precise role of DNA methylation in gastric cancer remains unclear.

Ras proteins play essential roles in controlling the activity of several important signaling pathways that regulate cellular proliferation, migration and apoptosis (11), and alteration of Ras signaling can lead to tumorigenesis. In fact, mutations of *K-ras* and *BRAF* have been observed in a number of human neoplasias (12,13), though their mutation rarely occurs in gastric cancer (14). Notably, activated forms of Ras also can induce senescence and apoptosis, indicating the presence of negative effectors regulated by Ras. Such effectors are commonly the products of RASSF family genes, and contain a Ras association (RA) domain. Alterations of these negative effectors of *Ras* also can play a role in tumorigenesis. For instance, epigenetic inactivation of *RASSF1*, a candidate tumor suppressor gene on chromosome 3p21, has been well characterized in a wide variety of tumors (15,16). So far, six members of the *RASSF* gene family, *RASSF1A*, *RASSF2A*, *RASSF4*, *RASSF5/NORE1*, *RASSF6* and *RASSF8*, have been shown to be inactivated or downregulated in human neoplasias (15–25). Of those, *RASSF2A* is frequently inactivated in colorectal, gastric, lung and nasopharyngeal cancers, although the molecular mechanisms by which RASSF2A functions as a tumor suppressor remains unknown (17,20,22,23,25).

In addition, *MST1* and *MST2* encode serine/threonine kinases that associate with RASSF family proteins (e.g. RASSF1 and RASSF5/*NORE1*) (26,27), and they are epigenetically inactivated in soft tissue sarcoma (28). The role of the RASSF/MST pathway in gastric cancer is not known, however.

In the present study, we examined the epigenetic alteration of *RASSF* family genes together with *MST1/2* in a panel of gastric cancer cell lines. We found that, of those, *RASSF2A* is the most frequently downregulated in gastric cancer. Introduction of RASSF2A into gastric cancer cells that do not otherwise express the gene significantly diminished colony formation and induced apoptosis. Induction of apoptosis by RASSF2A is associated with morphological changes and cytoplasmic localization of RASSF2A. Taken together, these findings suggest that epigenetic inactivation of *RASSF2A* plays a key role in tumorigenesis in gastric cancer.

Abbreviations: 5-aza-dC, 5-aza-2′-deoxycytidine; CIMP, CpG island methylator phenotype; NLS, nuclear localization signal; PCR, polymerase chain reaction; RA, Ras association.

[†]These authors contributed equally to this work.

Materials and methods

Cell lines and specimens

Twelve gastric cancer cell lines and 78 primary gastric cancer specimens were used in this study. Among the cell lines, eight were obtained from American Type Culture Collection, Tokyo, Japan or Japanese Collection of Research Bioresources Tokyo, Japan, whereas two (HSC44 and SH101) were kindly provided by Dr K.Yanagihara at the National Cancer Center Research Institute and were described previously (29,30). The 78 gastric cancer specimens were described previously (8,31). Written informed consent was obtained from every patient and approved by the Institutional Review Board. DNA was prepared using the standard phenol–chloroform method. Total RNA was isolated using Trizol (Invitrogen).

Reverse transcription–polymerase chain reaction

Five micrograms of total RNA were reverse transcribed using Superscript III reverse transcriptase (Invitrogen, Carlsbad, CA). Polymerase chain reaction (PCR) was carried out using primers specific for *RASSF2* exon 1A and exon 1B (supplementary Table 1 is available at *Carcinogenesis* Online). To analyze

restoration of RASSF2A, JRST, KatoIII, SNU1, SNU638 and HSC44 cells were incubated for 72 h with 2 μM 5-aza-2′-deoxycytidine (5-aza-dC) (Sigma, St Louis, MO). For quantitative real-time PCR, reactions were carried out using a 7900 Sequence Detection System (Applied Biosystems, Foster City, CA). The primers and probes for each gene are shown in supplementary Materials and Methods (available at *Carcinogenesis* Online). The relative levels of *RASSF2A* expression were quantified using the ΔCt value, which yields a ratio of the expression of a target gene to that of a housekeeping gene glyceraldehyde-3-phosphate dehydrogenase (GAPDH).

Bisulfite sequencing and pyrosequencing

Sodium bisulfite treatment was performed as described previously (32). The primer sequences and PCR parameters used are shown in supplementary Table 1 (available at *Carcinogenesis* Online). PCR products were cloned into pCR4.0 vector using a TOPO-TA Cloning Kit (Invitrogen). The sequencing reaction was carried out using a BigDye terminator cycle sequencing kit (PerkinElmer Biosystems, Foster city, CA), and sequencing was carried out using an ABI PRISM 3100 sequencer according to the manufacturer's guidelines (Applied Biosystems). Pyrosequencing was carried out as described previously (33,34), and the details are shown in supplementary Materials and Methods (available at *Carcinogenesis* Online).

Colony formation assay

An expression plasmid, pcDNA-*RASSF2A*, containing the entire coding region of human *RASSF2A* was constructed using the expression vector pcDNA3.1(+), which harbors a gene conferring geneticin resistance. Cells at 25% confluence in 10 cm dishes were transfected with 5 μg of one of three expression plasmids (pcDNA-*RASSF2A*, pcDNA-*RASSF2*-ΔRA or pcDNA3.1 control vector) using Nucleofector (Amaxa, Berlin, Germany) as described previously (17). Twenty-four hours after transfection, the cells were split 1:10 and grown for 14 days in the presence of G418 (Gibco BRL, Grand Island, NY) (0.3–0.6 mg/ml). The cells were then fixed and stained with Giemsa, and the number of colonies was scored. Experiments were performed in triplicate and repeated on two independent occasions.

Construction of adenoviral vectors and flow cytometry analysis

The generation, purification and infection procedures used with the replication-deficient recombinant adenovirus were described previously (35,36). For flow cytometric analysis, 1×10^6 cells were infected with an adenoviral vector containing RASSF2A (aa 1–326), RASSF2A-ΔN (aa 164–326), RASSF2A-ΔRA (aa 1–163), RASSF2A-ΔNLS (aa 1–149/168–326) or green fluorescent protein. The cells were then incubated for 24, 48 or 72 h, trypsinized, fixed with methanol, rehydrated with phosphate-buffered saline, treated with 2 mg/ml RNase for 30 min at 37°C and stained in 50 μg/ml propidium iodide solution. Fluorescence-activated cell sorting analysis was carried out using a Becton Dickinson FACScan flow cytometer (Braintree, MA).

Immunocytochemistry

Cells (1×10^4) were seeded on glass coverslips, infected with an adenoviral vector and fixed with 4% paraformaldehyde. Immunofluorescence analysis was carried out using mouse anti-Flag antibody and Alexa 488. For paxillin staining, the cells were incubated for 1 h with 0.1 μg/ml rhodamine-conjugated phalloidin (BD Bioscience, San Jose, CA). For Flag-RASSF2A staining, cells were incubated first with mouse anti-Flag monoclonal antibody (Sigma) and then with Alexa 488 goat anti-mouse antibody (Molecular Probes, Eugene, OR). Once labeled, the cells were examined under an Olympus IX71 fluorescence microscope. Nuclei were counterstained with 4′,6-diamidino-2-phenylindole.

Results

Epigenetic inactivation of RASSF family genes in gastric cancer cell lines

To determine the expression profile of negative effectors of Ras in gastric cancer, we examined the expression status of eight *RASSF* family genes plus *MST1* and *MST2* in a panel of gastric cancer cell lines. Of the 10 genes analyzed, the expression of RASSF2 was the most frequently downregulated in gastric cancer (Figure 1A). As a result of different transcription start sites, *RASSF2* has four major transcription variants: *RASSF2A* variant 1, *RASSF2A* variant 2, *RASSF2B* and *RASSF2C*. Analysis of the expression of each of these four isoforms revealed that both RASSF2A variants are expressed in all the normal tissues we tested (Figure 1B, upper panel). In contrast, their expression was lost in six gastric cancer cell lines (Figure 1B, lower panel) and, in MKN28 cells, expression of variant 1 was readily detected, but expression of variant 2 was very weak. Treating the gastric cancer cell lines with a methyltransferase inhibitor restored expression of the *RASSF2A* variants, indicating a role for DNA methylation in the silencing of *RASSF2A* expression (Figure 1C). Moreover, when we next examined *RASSF2* expression after treating cells with a low dose of 5-aza-dC and/or Trichostatin A(TSA), we found that treating HCC44 cells with 300 nM TSA or 0.2 μM 5-aza-dC had little effect on gene expression, but TSA plus 5-aza-dC acted synergistically to restore *RASSF2A* expression, which suggests the involvement of histone deacetylation in the gene's silencing (Figure 1D). Very little, if any, expression of *RASSF2B* and *RASSF2C* was detected (data not shown).

Aberrant methylation of RASSF2A in gastric cancer cell lines

To assess the role of DNA methylation in the silencing of *RASSF2A* in more detail, we used bisulfite sequencing to examine 37 CpG sites located around exons 1A and 1B of *RASSF2* in our panel of gastric cancer cell lines (Figure 1D). We detected high levels of methylation of exon 1A in JRST and KatoIII cells, which were consistent with the expression analysis. MKN28 cells showed high levels of methylation of exon 1B but not 1A, which are consistent with their expression of *RASSF2A* variant 1 and only a minimal amount of *RASSF2A* variant 2. Only sparse methylation was detected in MKN7, MKN74 and SH101 cells, which expressed the gene.

Effect of RASSF2A on cell growth and apoptosis in gastric cancer cells

To determine whether RASSF2A exerts an antiproliferative effect, we carried out a set of colony formation assays. Schematic representations of the various RASSF2 deletion constructs are shown in supplementary Figure 1 (available at *Carcinogenesis* Online). We found that introduction of RASSF2A into JRST and HSC44 cells resulted in a significant reduction of colony formation (Figure 2A and B). In contrast, a mutant form of RASSF2A that lacked the RA domain (ΔRA) was less able to suppress growth, indicating a role for the RA domain in suppression of cell growth. To investigate the role of RASSF2A-mediated inhibition of growth in more detail, we introduced Ad-*RASSF2A* into gastric cancer cell lines in which the gene was silenced. Transformation by Ad-*RASSF2A* induced apoptosis in JRST and SNU1 cells, which otherwise did not express *RASSF2A*, but did not induce apoptosis in cells that did express *RASSF2A*.

During the course of the experiments, we repeatedly noticed that RASSF2A transformants exhibited a round morphology, suggesting that *RASSF2A* expression leads to the inhibition Ras and, in turn, inhibition of focal adhesion and stress fiber formation and activation of paxillin. To test that idea, we used immunocytochemistry to examine paxillin expression (Figure 3A) and confirmed that the RASSF2A-induced round morphology was caused by the absence of stress fibers. We then examined whether these morphological changes induce apoptosis or whether it is apoptosis that induces the observed morphological changes. After transformation with Ad-*RASSF2A*, the numbers of floating cells increased, as did the incidence of apoptosis (Figure 3B). When we treated the cells with a non-specific caspase inhibitor, the number of floating cells increased, but the number of apoptotic cells decreased. This suggests that *RASSF2A* expression alters the morphology of cells, which leads first to a loss of adhesion and then to caspase-dependent apoptosis.

We next analyzed its protein motifs and found that RASSF2A carries three putative nuclear localization signals (NLSs) in the N-terminal region of its RA domain (NLS, ***RR***RGNVRTPSDQ***RRIRR***; start position, 150). Although RASSF2A expressed in JRST cells was localized in both the nucleus and cytoplasm, RASSF2A lacking the NLS (RASSF2A-ΔNLS) was found only in the cytoplasm, indicating its NLS is a key determinant of the intracellular distribution of RASSF2A (Figure 4A). Interestingly, when introduced into cells, RASSF2A-ΔNLS exerted a strong proapoptotic effect (Figure 4B).

Identification of genes induced by RASSF2A

To learn more about the molecular pathway via which RASSF2A suppresses cell growth and induces apoptosis, we used